Takens-Bogdanov bifurcations without parameters, and oscillatory shock profiles

Bernold Fiedler and Stefan Liebscher

Free University Berlin
Institute of Mathematics I
Arnimallee 2-6
D–14195 Berlin
Germany

fiedler@math.fu-berlin.de, liebsch@math.fu-berlin.de
http://www.math.fu-berlin.de/~Dynamik/

January 2001

To appear in
H.W. Broer, B. Krauskopf, and G. Vegter, editors
Global Analysis of Dynamical Systems
Festschrift dedicated to Floris Takens for his 60th birthday
To be published by IOP, 2001

1 Introduction and examples

Bifurcation theory deals with the dynamics associated to vector fields

$$\begin{aligned} \dot{\mathbf{x}} &= f^{\mathrm{x}}(\mathbf{x}, \lambda) \\ \dot{\lambda} &= 0 \end{aligned} \tag{1.1}$$

which depend on one or several real parameters $\lambda \in \mathbb{R}^m$. Mostly the analysis is local in λ. Moreover $\mathbf{x} \in \mathbb{R}^n$, or $\mathbf{x}$ in an n-dimensional manifold, is near a fairly simple time invariant object. See for example [CH82], [GSS85], [GSS88], [GH82], [HK91], [Kuz95], and the many references there. Frequently, for example, it is assumed that

$$0 = f^{\mathrm{x}}(0, \lambda) \tag{1.2}$$

so that $\mathbf{x} = 0$ is a given "trivial", or "primary" equilibrium solution, independently of the parameter λ. Clearly this gives rise to a manifold of trivial equilibria of dimension $m = \dim \lambda$. In addition, the equation $\dot{\lambda} = 0$ trivially provides an invariant foliation $\lambda =$ constant of phase space $(\mathbf{x}, \lambda)$, transverse to the equilibrium manifold $(0, \lambda)$.

In the present paper, we abandon this foliation by constant parameter values λ, but keep the requirement of a trivial equilibrium manifold in effect. Replacing λ by $\mathbf{y} \in \mathbb{R}^m$ to mark that difference we consider

$$\begin{aligned} \dot{\mathbf{x}} &= f^{\mathrm{x}}(\mathbf{x}, \mathbf{y}) \\ \dot{\mathbf{y}} &= f^{\mathrm{y}}(\mathbf{x}, \mathbf{y}) \end{aligned} \tag{1.3}$$

with the convenient abbreviation $\dot{z} = f(z)$, where $z = (\mathbf{x}, \mathbf{y})$ and $f = (f^{\mathrm{x}}, f^{\mathrm{y}})$. As before, we assume the existence of a manifold of trivial equilibria

$$0 = f(0, \mathbf{y}) \tag{1.4}$$

for all $\mathbf{y} \in \mathbb{R}^m$. We also assume $f \in C^\kappa$ to be sufficiently smooth, throughout; $\kappa \geq 5$ is more than enough.

The celebrated Takens-Bogdanov bifurcation deals with (1.1) for two real parameters $\lambda = (\lambda_1, \lambda_2) \in \mathbb{R}^2$ and under the (generic) assumption of an algebraically double zero eigenvalue

$$\mathrm{D}_{\mathbf{x}} f^{\mathrm{x}}(\mathbf{x} = 0, \lambda = 0) = \begin{pmatrix} 0 & 0 \\ 1 & 0 \end{pmatrix}, \tag{1.5}$$

see [Arn72], [Tak73], [Tak74], [Bog76a, Bog76b], and also [Bog81a, Bog81b]. For more recent accounts see also [GH82], [Arn83]. The standard unfolding in parameter space $\lambda = (\lambda_1, \lambda_2)$ involves a curve of stationary saddle-node bifurcations, and half-arcs of Hopf

bifurcations and homoclinic orbits, respectively. In the present paper, in contrast, we will drop the foliation $\dot\lambda = 0$, but treat (1.3), (1.4) with $\mathbf{x}, \mathbf{y} \in \mathbb{R}^2$ and a nilpotent linearization (1.5) in complete analogy to the celebrated Takens-Bogdanov bifurcation.

We contend that the problem of bifurcation from manifolds of equilibria, even in absence of any parameter foliations $\dot\lambda = 0$, and degenerate as it may seem, arises quite naturally in applications. We give three examples next. For further details we refer to section 12 below, as well as to [AA86], [AF89], [Far84], [Lie97], [Lie00], [FLA00a], [FL00], [FLA00b].

Example 1.1 Our first example arises in *population dynamics, game theory etc.*; see also [Far84]. For $\mathbf{x} = (x_1, \ldots, x_n) \in \mathbb{R}^n_+$ let B be a degenerate real $(n \times n)$-matrix, say with one-dimensional right/left kernel spanned by $\mathbf{r}, \mathbf{l} \in \mathbb{R}^n$, respectively. Consider the system

$$\dot x_j \;=\; x_j \cdot ((B\mathbf{x})_j - b_j), \tag{1.6}$$

$j = 1, \ldots, n$. For $\mathbf{b} = (b_1, \ldots, b_n) \in \text{range } B$, we obtain a line of equilibria

$$\mathbf{x} \;=\; \mathbf{x}^0 + y \cdot \mathbf{r}, \qquad y \in \mathbb{R}, \tag{1.7}$$

which may intersect the positive orthant. Analysis is facilitated, in this example, by the presence of a first integral (alias, conserved quantity) given by $\prod_j x^{l_j}$. Higher-dimensional kernels of B may clearly give rise to higher-dimensional equilibrium subspaces.

Example 1.2 Our second example arises in the study of *viscous profiles* of nonlinear hyperbolic conservation laws, mixed with stiff balance laws. We consider travelling wave solutions $u(t, \xi) = U(\varepsilon^{-1}(\xi - st))$ of systems

$$\partial_t u + \partial_\xi F(u) \;=\; \varepsilon^{-1} G(u) + \varepsilon\delta\partial_\xi^2 u, \tag{1.8}$$

where $\varepsilon \searrow 0$ indicates a small parameter. The associated travelling wave system is independent of ε and reads

$$\delta U'' + (sU - F(U))' + G(U) \;=\; 0 \tag{1.9}$$

The case of vanishing $G(u) \equiv 0$ of pure conservation laws has been studied most widely; see for example [Smo94]. Putting $z = (U, U')$, we obtain a trivial equilibrium manifold $(U, 0)$ of dimension $\dim U = \frac{1}{2} \dim z$. Heteroclinic solutions which converge to different limits $(u_\pm, 0)$ in this manifold, for time tending to $\pm\infty$, are called viscous shock profiles of the Riemann problem with Riemann data $u_\pm$. Indeed, the solution $U(\varepsilon^{-1}(\xi - st))$ then converges in the limit $\varepsilon \searrow 0$ to a discontinuous weak solution of (1.8), a shock, which propagates at constant speed s. Analysis is greatly facilitated by the first integrals

$$\delta U' + sU - F(U) \;\equiv\; \text{constant}, \tag{1.10}$$

in this case.

The opposite extreme where $G(u) = 0$ only holds for isolated points u does not give rise to equilibrium manifolds of positive dimension. A typical case, however, arises when some — but not all — components $G_j(u)$ vanish identically. This corresponds to conservation laws for some components u_j, whereas the remaining u-components encounter source terms. As a consequence the equilibrium system

$$G(u) \;=\; 0 \tag{1.11}$$

becomes under-determined, and equilibrium manifolds $z = (u, 0) \in M$ usually appear. The dimension m of M will typically be given by the number of conservation laws. For detailed analysis of the case of single conservation laws, alias lines of equilibria, see [Lie97], [Lie00], [FLA00a], [FL00], [FLA00b], as well as sections 2, 12 below. We explicitly mention the appearance of linearly stable weak viscous shock-profiles, which violate the Lax entropy condition and are oscillatory — in marked contrast to the case $G \equiv 0$ of pure conservation laws.

Example 1.3 Our third example is based on an observation for *coupled oscillators* due to [AA86], see also [AF89], [Lie97], [FLA00b]. Let $i \in \{\pm 1, \ldots, \pm(m+1)\}$ denote the vertices of an $(m+1)$-dimensional 2^{m+1}-hedron C. The neighbors $\mathcal{N}_i$ of vertex i are all i', except i itself and $-i$. Consider the coupled system

$$\dot{u}_i \;=\; F\left(u_i, \sum_{i' \in \mathcal{N}_i} u_{i'}\right). \tag{1.12}$$

If $F(\cdot, 0)$ is odd, $F(-u, 0) = -F(u, 0)$, then the coupled oscillator system (1.12) possesses an invariant subspace, where the dynamics is described by an $(m+1)$-fold direct product of the uncoupled flows

$$\dot{u} \;=\; F(u, 0). \tag{1.13}$$

Indeed the subspace given by

$$u_{-i} \;=\; -u_i, \tag{1.14}$$

for all i, is invariant and eliminates any coupling. For examples on graphs more intricate than C see [AF89].

Suppose the uncoupled dynamics (1.13) possess a periodic orbit. This gives rise to an $(m+1)$-dimensional invariant torus of the coupled system (1.12), foliated by periodic orbits. In a (local) Poincaré cross section the torus manifests itself as an m-dimensional manifold M of fixed points. As was pointed out by [Tak73], in normal form up to any finite order this Poincaré map (or its second iterate) coincides with the time-one map of

an autonomous vector field in the Poincaré cross section; see [BT89]. The manifold M of fixed points then becomes a manifold M of equilibria.

Alternatively, we may assume equivariance of F under an S^1-action such that the periodic orbits of (1.13) become group orbits alias rotating waves under this action. Then the full vector field (1.12) pulls back to a vector field in the Poincaré section, by the Palais construction, and the Poincaré map coincides with the time one map of the pulled back vector field. See for example [AF89], and for the Palais construction [FSSW96]. Again, the manifold M of fixed points becomes an equilibrium manifold.

Sufficiently motivated, as we now are, to consider vector fields with equilibrium manifolds M of dimension m, the paper is organized as follows. In section 2, we recall some basic results on the case of equilibrium lines, $m = 1$. The simplest case of a nontrivial eigenvalue zero, in the linearization, is addressed, as well as the two cases of Hopf bifurcation without parameters, caused by purely imaginary eigenvalues. Section 3 lists several possibilities for bifurcations from equilibrium planes, $m = 2$ — among them, most notably, the Takens-Bogdanov bifurcation without parameters. Focussing on only this case for the rest of this paper, we briefly discuss the relevant normal form which preserves the equilibrium plane; see section 4. In section 5, a suitable scaling provides an expansion in an artificial small blow-up parameter ε. To leading order ε^0, the resulting scaled system becomes completely integrable, in section 6, though not quite Hamiltonian. The resulting slow flow of first integrals, at order ε^1, is derived in section 7, relegating discussions of elliptic integrals to section 8. Resorting to some numerical evaluation of Weierstrass functions, at last, this analysis remains incomplete. "Averaging" of the rapid oscillations in the slow flow is performed in section 9. Before we draw geometric conclusions on the three essentially different types of Takens-Bogdanov bifurcations without parameters, in section 11, we stroll the landscape of averaging, subharmonic resonance, Melnikov functions, truncation of normal forms and discretization of the "averaged" vector field, in section 10. We conclude, in section 12, with an explicit example of stiff balance laws, which exhibits all three types of Takens-Bogdanov bifurcations without parameters which are derived in this paper.

Acknowledgements

We are indebted to Abderrahim Azouani, Henk Broer, Sebius Doedel, Vassili Gelfreich, Ale Jan Homburg, Oliver Junge, Arnd Scheel, Dmitry Turaev for valuable comments during preparation of this paper. All expert typesetting was accomplished by Regina Löhr. And without guidance by the pioneering papers of Floris Takens, written more than 25 years ago, this paper could not have been written.

2 Bifurcations from lines of equilibria

As a preparation for our investigation of Takens-Bogdanov bifurcations from planes of equilibria, in section 3, we first recall earlier results on bifurcations from lines of equilibria. We begin with the case of normal hyperbolicity of the equilibrium line, and then proceed to address the occurrence of a nontrivial zero eigenvalue as well as purely imaginary eigenvalues. In classical bifurcation theory, characterized by a foliation $\dot\lambda = 0$ by a scalar parameter $\lambda \in \mathbb{R}$, these latter cases would correspond to bifurcation of nontrivial equilibria and to Hopf bifurcation of small amplitude periodic oscillations, respectively.

In the notation of (1.3), (1.4) we consider vector fields

$$\begin{aligned} \dot{\mathbf{x}} &= f^{\mathrm{x}}(\mathbf{x}, y) \\ \dot y &= f^{\mathrm{y}}(\mathbf{x}, y) \end{aligned} \tag{2.1}$$

with $\mathbf{x} \in \mathbb{R}^n$, scalar $y \in \mathbb{R}$ replacing the parameter λ, and a trivial line of equilibria

$$0 = f(0, y) \tag{2.2}$$

of the vector field $f = (f^{\mathrm{x}}, f^{\mathrm{y}})$. In block matrix notation, the linearization $A(y)$ of f at the equilibrium $(0, y) \in \mathbb{R}^{n+1}$ is given by

$$A(y) = \begin{pmatrix} A_0(y) & 0 \\ & 0 \end{pmatrix}, \tag{2.3}$$

with the normal part $A_0(y) := \mathrm{D}_{\mathbf{x}} f^{\mathrm{x}}(0, y)$. The spectrum of $A(y)$ is given by

$$\operatorname{spec} A(y) = \{0\} \cup \operatorname{spec} A_0(y), \tag{2.4}$$

just adding a (trivial) eigenvalue zero to the spectrum of the linearization $A_0(y)$ normal to the equilibrium line.

Normal hyperbolicity simply requires all eigenvalues of $A_0(y)$ to possess nonzero real part. Standard theory of normal hyperbolicity then identifies a local *center-stable manifold* W^{cs} of the equilibrium line which consists of all initial conditions $(\mathbf{x}^0, y^0) \in \mathbb{R}^{n+1}$ near $\{0\} \times \mathbb{R}$, such that $\mathbf{x}(t)$ remains small for all positive times t. The center-stable manifold W^{cs} is foliated by the *strong stable manifolds* $W^{\mathrm{ss}}(y)$ of those $(\mathbf{x}^0, y^0) \in \mathbb{R}^{n+1}$ near $\{0\} \times \mathbb{R}$ selected by the additional requirement

$$\lim_{t \to +\infty} (\mathbf{x}(t), y(t)) = (0, y). \tag{2.5}$$

Similarly, but going backwards in time instead, we obtain the foliation of the *center-unstable manifold* W^{cu} by *strong unstable manifolds* $W^{\mathrm{uu}}(y)$. See for example [HPS77],

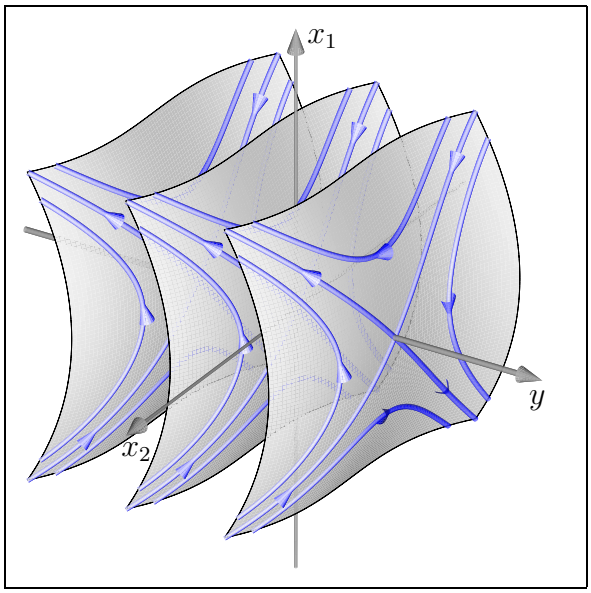

Figure 2.1: A normally hyperbolic line of equilibria with flow-invariant foliation.

[Fen77, Fen79], [Aul84] for additional background and technical details. Tangent spaces to $W^{\mathrm{ss}}(y)$ and $W^{\mathrm{uu}}(y)$ at $(0, y)$, for example, are given by the eigenspaces of $A(y)$ corresponding to the spectrum strictly in the left and right complex half plane, respectively. By (2.4), these eigenvalues are precisely the eigenvalues of the normal part $A_0(y)$.

An interesting generalization of the Grobman-Hartman theorem to the case of non-hyperbolic equilibria has been proved by [Sho75]; see [Arn83]: locally, the flow is given as a direct product of the linearized hyperbolic part with the flow in the center manifold W^{c}, up to C^0 flow equivalence. Applied to our case, where $W^{\mathrm{c}} = W^{\mathrm{cs}} \cap W^{\mathrm{cu}}$ is just the equilibrium line, this reduces the flow to

$$\begin{aligned} \dot{\mathbf{x}} &= A_0(y)\mathbf{x} \\ \dot{y} &= 0. \end{aligned} \tag{2.6}$$

Note that y has in fact become a parameter, in these coordinates. See figure 2.1 for a phase portrait.

We consider the two generic possibilities of a non-hyperbolic normal part $A_0(y)$ next: a simple (nontrivial) eigenvalue zero, and a simple purely imaginary pair $\pm\mathrm{i}$, respectively, which cross the imaginary axis at nonzero speed, as y increases through $y = 0$. Eliminating the foliations due to the remaining hyperbolic part of $A_0(0)$, we reduce our attention to the center manifold and only consider $\mathbf{x} = x \in \mathbb{R}$, $\mathbf{x} = (x_1, x_2) \in \mathbb{R}^2$, respectively.

For the case of a simple eigenvalue zero, where $\mathbf{x} = x \in \mathbb{R}$, see [Lie97], [DR98].

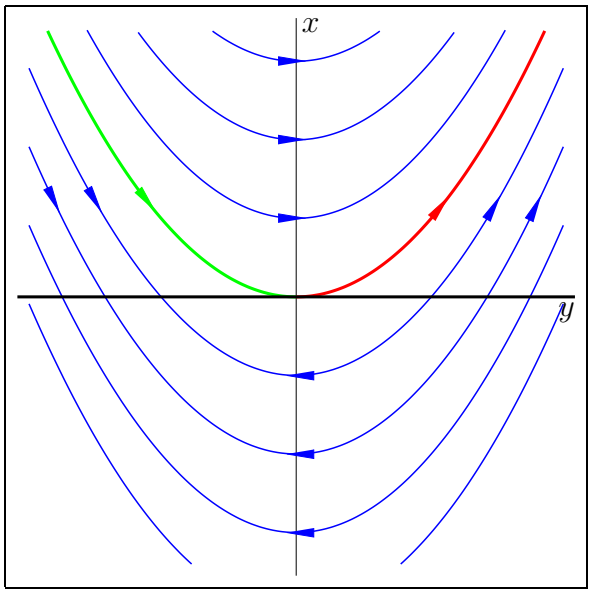

Figure 2.2: Phase portrait of failure of normal hyperbolicity due to a nontrivial simple eigenvalue zero, at $y = 0$.

Since $f(0, y) \equiv 0$, we can divide by x and obtain

$$\dot{z} \quad = \quad x\tilde{f}(z) \tag{2.7}$$

for $z = (x, y) \in \mathbb{R}^2$. Dividing by the Euler multiplier x, which reverses time for $x < 0$, we obtain the time orbits of (2.7) from the time orbits of

$$z' \quad = \quad \tilde{f}(z). \tag{2.8}$$

Invoking a flow box theorem for (2.8), adapted to preserve the straight equilibrium line, reduces (2.7) to

$$\begin{aligned} \dot{x} &= axy \\ \dot{y} &= x. \end{aligned} \tag{2.9}$$

Note the normal part of the linearization

$$A_0(y) \quad = \quad \mathrm{D_x} f^{\mathrm{x}}(0, y) \quad = \quad ay \tag{2.10}$$

and $a \neq 0$, by transverse crossing of the zero "eigenvalue" ay of $A_0(y)$ at $y = 0$. To avoid the case $\dot{y} = f^{\mathrm{y}}(z) \equiv 0$ of a trivial foliation with "ordinary" bifurcation parameter y, the nondegeneracy condition $\mathrm{D_z} f^{\mathrm{y}}(0, 0) \neq 0$ has to be imposed on (2.7). Since $f^{\mathrm{y}}(0, y) \equiv 0$ and hence $\mathrm{D_y} f^{\mathrm{y}}(0, 0) = 0$ we obtain $\mathrm{D_x} f^{\mathrm{y}}(0, 0) \neq 0$, which accounts for the y-component of (2.9). See figure 2.2 for a phase portrait with $a = 1$. Note the absence of nontrivial equilibria and the heteroclinic orbits in the lower half plane $x < 0$.

The case of purely imaginary eigenvalues $y \pm \mathrm{i}$, at $y = 0$, of the normal part linearization $A_0(y)$ leads to a normal form

$$\begin{array}{rcl} \dot{r} &=& ry \\ \dot{y} &=& \frac{1}{2}ar^2 \\ \dot{\varphi} &=& 1 \end{array} \tag{2.11}$$

in polar coordinates $x_1 + \mathrm{i}x_2 = re^{\mathrm{i}\varphi}$ for $\mathbf{x} = (x_1, x_2) \in \mathbb{R}^2$. We have used the purely imaginary Hopf eigenvalues $\pm\mathrm{i}$ at $y = 0$ to eliminate dependence on φ, in normal form, and we have truncated at second order. For a technically more careful discussion, we refer to [FLA00a]. This result was used by [DR98] to illustrate a more general blow-up procedure. Division by the Euler multiplier r leads to the linear system

$$\begin{array}{rcl} \dot{r} &=& y \\ \dot{y} &=& \frac{1}{2}ar \end{array} \tag{2.12}$$

We distinguish the *elliptic* case, $a < 0$, and the *hyperbolic* case, $a > 0$. The elliptic case was already studied by [Far84], see also [FLA00a], [FL00], [FLA00b], [Lie00].

In normal form, truncated at any finite order, the flow reduces to (2.11), with all orbits spiraling along ellipsoids in the elliptic case, or cones and hyperboloids, in the hyperbolic case. See figure 2.3.

Note how all nonstationary orbits leave a neighborhood of the equilibrium line in either forward or backward time, in the hyperbolic case. This observation remains true when we include higher order terms not in normal form.

In the elliptic case, such higher order terms may split the ellipsoids in a transverse way. Due to results of Neishtadt type [Nei84], the splittings will be exponentially small in terms of the size of the ellipsoid, in the analytic case; see also [BR01], [FS96], [Gel99], [GL01], and the references there. Note the absence of periodic orbits. In fact, any nonstationary orbit is heteroclinic from an equilibrium $y_- > 0$ to an equilibrium $y_+ < 0$, locally. The set of all ω-limiting equilibria y_+ which occur in any fixed, two dimensional strong unstable manifold $W^{\mathrm{uu}}(y_-)$ may cover a closed interval in $(-\infty, 0)$, however, due to Neishtadt splitting.

Still, the system possesses a smooth Lyapunov function $V = V(\mathbf{x}, y)$, in the elliptic case, which decreases strictly along all trajectories. We give one possible construction. It turns out that all nonstationary orbits cross the $\mathbf{x}$-plane $y = 0$, and do so transversely; see [FLA00a], proposition 2.1. Normalizing time to $t = 0$, at this crossing, we define

$$V(\mathbf{x}(t), y(t)) \;:=\; p(\tanh t; y_-, y_+) \tag{2.13}$$

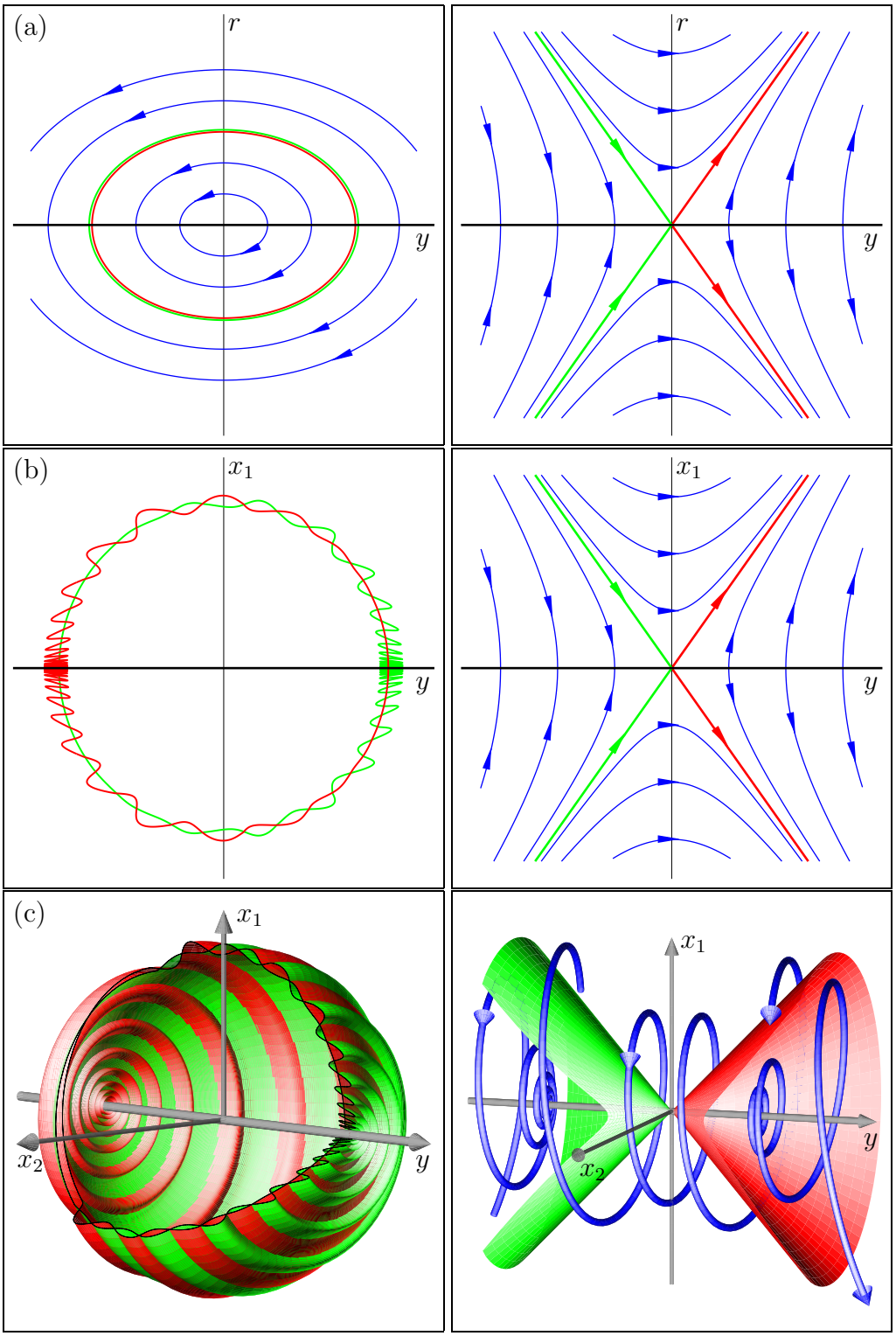

Figure 2.3: Hopf bifurcation from lines of equilibria without parameters; elliptic case (left) and hyperbolic case (right). Normal form (a), Poincaré section $x_2 = 0$ (b), and three-dimensional views.

where $p(\tau; y_-, y_+)$ is the unique parabola in τ mapping the three τ-values $(-1, 0, +1)$ to $(y_-, 0, y_+)$, and $y_\pm = \lim_{t\to\pm\infty} y(t)$ depend on the specific trajectory. Then $V(\mathbf{x}, 0) = 0$, $V(0, y) = y$, and V is a smooth Lyapunov function.

Just as the classical Takens-Bogdanov bifurcation in two parameters requires an understanding of stationary and Hopf bifurcations, in one parameter, all the above examples for bifurcations along lines of equilibria, without parameters, will contribute to the three types of Takens-Bogdanov bifurcations from an equilibrium plane presented in the next section.

3 Bifurcations from planes of equilibria

We now proceed to an analysis of planes of equilibria arising in vector fields

$$\begin{aligned} \dot{\mathbf{x}} &= f^{\mathrm{x}}(\mathbf{x}, \mathbf{y}) \\ \dot{\mathbf{y}} &= f^{\mathrm{y}}(\mathbf{x}, \mathbf{y}) \end{aligned} \tag{3.1}$$

where $\mathbf{x} \in \mathbb{R}^n$, $\mathbf{y} = (y_1, y_2) \in \mathbb{R}^2$ and $f = (f^{\mathrm{x}}, f^{\mathrm{y}})$ satisfies

$$0 = f(0, \mathbf{y}), \tag{3.2}$$

for all $\mathbf{y}$. As before, we have a block matrix decomposition of the linearization

$$A(\mathbf{y}) = \mathrm{D}_{\mathrm{z}} f(0, \mathbf{y}) = \begin{pmatrix} A_0(\mathbf{y}) & 0 \\ A_1(\mathbf{y}) & 0 \end{pmatrix}, \tag{3.3}$$

with families of real $(2 \times n)$-matrices $A_1(\mathbf{y})$ parametrized by $\mathbf{y} \in \mathbb{R}^2$. For the normal part $A_0(\mathbf{y})$, which determines the nontrivial spectrum of $A(\mathbf{y})$, several nonhyperbolic cases arise in generic two-parameter families; see the cases in [Tak73] and the discussion in [Arn83]. Specifically, $A_0(0)$ can possess

(a) a simple eigenvalue zero

(b) a pair of simple, purely imaginary eigenvalues (Hopf)

(c) an algebraically double, geometrically simple eigenvalue zero (Takens-Bogdanov)

(d) both (a) and (b) (zero-Hopf)

(e) two nonresonant pairs of simple, purely imaginary eigenvalues (Hopf-Hopf)

Clearly (a), (b) will then occur along curves in $\mathbf{y}$-space, unless additional degeneracy conditions like non-transverse eigenvalue crossings or degeneracy of other higher order

terms are imposed. Cases (c)–(e), in contrast, possess codimension two in the space of $(n \times n)$-matrices $A_0(\mathbf{y})$ and hence will generically occur at isolated values of $\mathbf{y} \in \mathbb{R}^2$, say at $\mathbf{y} = 0$.

As a diversion, we also note a hybrid between "ordinary" bifurcation theory, where $\dot{\lambda} = 0$, and on the other hand (3.1), (3.2), which fix only the y-plane $\mathbf{x} = 0$. Let $f^{\mathrm{y}} = (f^{\mathrm{y}_1}, f^{\mathrm{y}_2})$ and assume

$$0 \equiv f^{\mathrm{y}_2}(\mathbf{x}, \mathbf{y}) \tag{3.4}$$

for all $(\mathbf{x}, \mathbf{y}) \in \mathbb{R}^{n+2}$. Then $\dot{y}_2 = 0$, and y_2 becomes an "ordinary" bifurcation parameter. Writing $\mathbf{y} = (y, \lambda)$ with $y, \lambda \in \mathbb{R}$, in this case, we then have to discuss systems of the form

$$\begin{aligned} \dot{\mathbf{x}} &= f^{\mathrm{x}}(\mathbf{x}, y, \lambda) \\ \dot{y} &= f^{\mathrm{y}}(\mathbf{x}, y, \lambda) \end{aligned} \tag{3.5}$$

where $f(0, y, \lambda) \equiv 0$. These vector fields are just one-parameter versions of systems with trivial equilibrium *lines*, as discussed in section 2, see (2.1), (2.2). For fixed λ, for example, cases (a) and (b) were discussed in section 2. In fact, (b) gave rise to two distinct cases of Hopf bifurcation without parameters which we called elliptic and hyperbolic. Varying λ, cases (d) and (e) can then be viewed as the collision of cases (a)-(b), and (b)-(b), respectively. Similarly, as we will see below, the Takens-Bogdanov case (c) can arise from the Hopf case (b) if the Hopf frequency tends to zero as the parameter λ varies. The half-arc of Hopf bifurcation points, in the (y, λ)-plane, then terminates at a nilpotent Jordan block A_0.

In this paper, we henceforth restrict to the Takens-Bogdanov case (c), where $A_0(0)$ is nilpotent. We now summarize some main results. Under suitable nondegeneracy conditions, we may choose local coordinates (y_1, y_2) such that $A_0(\mathbf{y})$, $A_1(\mathbf{y})$, take the form

$$A_0(\mathbf{y}) = \begin{pmatrix} a(-y_1 + y_2) & -y_1 \\ 1 & 0 \end{pmatrix} \tag{3.6}$$

$$A_1(\mathbf{y}) = \begin{pmatrix} (c_1 y_1 + c_2 y_2) & 1 \\ c_3(c_1 y_1 + c_2 y_2) & 0 \end{pmatrix} \tag{3.7}$$

for some $a \neq 0$. For details we refer to our discussion of normal forms in section 4. Again we have omitted the hyperbolic part of A_0, so that $\mathbf{x} = (x_1, x_2) \in \mathbb{R}^2$. Note that we may, and do, assume $a > 0$ if we allow for linear transformations of $\mathbf{x}, \mathbf{y}$ and for a reversal of time. In fact we will absorb a completely into the scaling, alias blow-up (5.2) below. Note

the Jordan block of order 3 in the full linearization

$$A(\mathbf{y}) \;=\; \begin{pmatrix} A_0(0) & 0 \\ A_1(0) & 0 \end{pmatrix} \;=\; \begin{pmatrix} 0 & 0 & 0 & 0 \\ 1 & 0 & 0 & 0 \\ 0 & 1 & 0 & 0 \\ 0 & 0 & 0 & 0 \end{pmatrix} \tag{3.8}$$

at $\mathbf{y} = 0$.

A normal form of the vector field $\dot{z} = f(z)$ up to second order in $z = (\mathbf{x}, \mathbf{y})$ reads as follows:

$$\begin{aligned} \dot{x}_1 &= a x_1(-y_1 + y_2) - x_2 y_1 + a b x_2^2 \\ \dot{x}_2 &= x_1 \\ \dot{y}_1 &= x_2 + x_1(c_1 y_1 + c_2 y_2) \\ \dot{y}_2 &= c_3 x_1(c_1 y_1 + c_2 y_2). \end{aligned} \tag{3.9}$$

In the following sections 5–11, we use a blow-up or scaling reminiscent of the classical Takens-Bogdanov bifurcation, to exhibit features of the truncated system (3.9), locally near $\mathbf{x} = \mathbf{y} = 0$, which survive the addition of higher order terms. Some of these features, which are the main result of this paper, can be summarized as follows.

Let $b \notin \{-17/12, -1\}$. Then there exists a neighborhood U of $\mathbf{x} = \mathbf{y} = 0$ in $\mathbb{R}^4$ such that any trajectory $(\mathbf{x}(t), \mathbf{y}(t))$ which remains in U, be it for all positive or all negative times, converges to some equilibrium $(0, \mathbf{y})$, in the trivial equilibrium plane $\mathbf{x} = 0$. More specifically, let $z(t) = (\mathbf{x}(t), \mathbf{y}(t)) \in U$ for all $t \geq 0$. Then $\lim \mathbf{x}(t) = 0$, for $t \to +\infty$, and there exists

$$\mathbf{y}_+ \;:=\; \lim_{t \to +\infty} \mathbf{y}(t). \tag{3.10}$$

Similarly, $z(t) \in U$ for all $t \leq 0$ implies $\lim \mathbf{x}(t) = 0$, for $t \to -\infty$, and

$$\mathbf{y}_- \;:=\; \lim_{t \to -\infty} \mathbf{y}(t) \tag{3.11}$$

exists. Of course, nonstationary heteroclinic orbits which remain in U for all $t \in \mathbb{R}$ and for which both (3.10) and (3.11) hold, are possible, albeit with $\mathbf{y}_+ \neq \mathbf{y}_-$. In particular, U is void of nontrivial equilibria, of periodic orbits, and of any homoclinic orbits. Any orbit which remains in U, for all times $t \in \mathbb{R}$, is stationary or heteroclinic.

In figure 3.1 we depict the three essentially different cases which arise in the three parameter regions

$$\begin{aligned} &\text{Case (A)} && b < -17/12 \\ &\text{Case (B)} && -17/12 < b < -1 \\ &\text{Case (C)} && -1 < b \end{aligned}$$

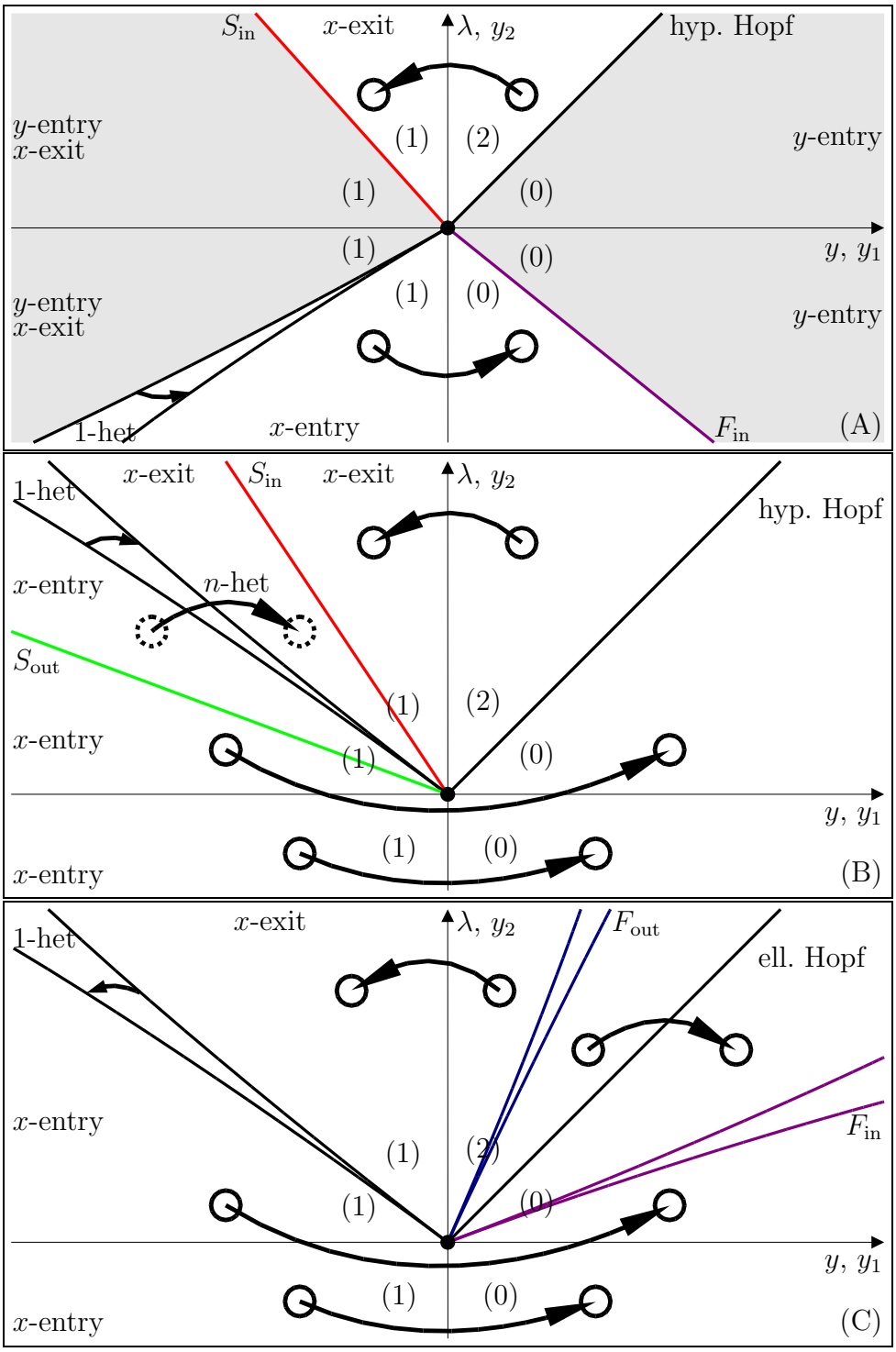

Figure 3.1: Three cases of Takens-Bogdanov bifurcations without parameters, see (3.9) and (A)–(C) for coefficients. Unstable dimensions i of trivial equilibria $(0, \mathbf{y})$ are indicated by (i); "n-het" indicate saddle-saddle heteroclinics with n revolutions around the positive y_1-axis. See sections 9,11 for a detailed description.

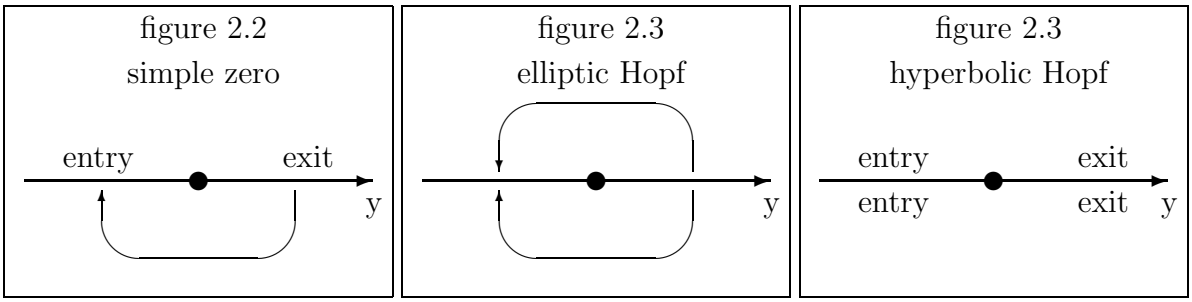

Figure 3.2: Schematic diagrams of bifurcations from lines of equilibria.

Arrows indicate the pairings $(y_- \mapsto y_+)$ by heteroclinic orbits. We also indicate *exit sets*, for which the strong unstable manifolds $W^{\rm uu}(y)$ leave U in forward time, at least partially, as well as *entry sets*, where $W^{\rm ss}(y)$ shares the same fate in backwards time. The difference between "x-entry/exit" and "y-entry/exit" will be explained in sections 9–11.

It is interesting to note that these diagrams do not depend on the values of c_1, c_2, c_3, to leading order; see the blow-up construction in section 5. In particular, we may choose $c_1 = c_2 = 0$. This identifies y_2 as a parameter, to leading order, by $\dot{y}_2 = 0$. Writing $y_1 = y$, $y_2 = \lambda$ as in diversion (3.4), (3.5) above, we can equivalently view the Takens-Bogdanov bifurcations without parameters as a termination of Hopf bifurcation from a line of equilibria given by the y-axis, as an external parameter λ is varied. In this setting, both the elliptic and the hyperbolic Hopf case arise, as discussed in section 2.

Although figure 3.1 gives an indication of heteroclinicity, it does not reveal the detailed geometry of the associated flows of $(\mathbf{x}, y) \in \mathbb{R}^3$, as parametrized by $\lambda \in \mathbb{R}$. In fact the results of figures 2.2, 2.3 would be represented quite schematically by figure 3.2. All geometric intricacies are lost, like $W^{\rm uu}(y_-)$ terminating at y_+-intervals in the elliptic Hopf case, or distinctions between saddle-saddle heteroclinics, saddle-node heteroclinics, and focus-node heteroclinics. For some such geometric detail we refer to section 11 below.

4 Normal forms

In this section we consider

$$\begin{aligned} \dot{\mathbf{x}} &= f^{\mathrm{x}}(\mathbf{x},\mathbf{y}) \\ \dot{\mathbf{y}} &= f^{\mathrm{y}}(\mathbf{x},\mathbf{y}) \end{aligned} \tag{4.1}$$

with $\mathbf{x},\mathbf{y} \in \mathbb{R}^2$, an equilibrium plane

$$0 = f(0,\mathbf{y}), \tag{4.2}$$

and nilpotent normal part linearization

$$A_0(0) = \mathrm{D}_{\mathbf{x}} f^{\mathrm{x}}(0,0) = \begin{pmatrix} 0 & 0 \\ 1 & 0 \end{pmatrix}. \tag{4.3}$$

For terms up to order 2 in $\mathbf{x},\mathbf{y}$, we derive the normal form (3.9) such that the $\mathbf{y}$-plane $\mathbf{x}=0$ remains an equilibrium plane.

As a first step we consider the appropriately nondegenerate linearization

$$A(0) = \begin{pmatrix} A_0(0) & 0 \\ A_1(0) & 0 \end{pmatrix} = \begin{pmatrix} 0 & 0 & 0 & 0 \\ 1 & 0 & 0 & 0 \\ A_1(0) & & 0 & 0 \\ & & 0 & 0 \end{pmatrix} \tag{4.4}$$

at $\mathbf{x}=\mathbf{y}=0$. The nondegeneracy which we choose for $A_1(0)$ is such as can occur in generic two-parameter families of linearizations $A(\mathbf{y})$ subject to the equilibrium constraint (4.2). We fix $\mathbf{y}=0$ by requiring nilpotency of $A_0(0)$. Because the $\mathbf{y}$-plane $\mathbf{x}=0$ is distinguished to be an equilibrium plane, we may consider

$$\operatorname{range} A(0) \cap \{\mathbf{x}=0\} \tag{4.5}$$

as an invariant object. With a two-dimensional kernel of $A(0)$ at hand, generically, and one dimension of range $A(0)$ fixed as the x_2-axis, by $A_0(0)$, the space (4.5) is one-dimensional: call it the y_1-axis. Therefore $A_1(0)$ takes the form

$$A_1(0) = \begin{pmatrix} \alpha & 1 \\ 0 & 0 \end{pmatrix}, \tag{4.6}$$

generically with a nonzero upper right entry which we have normalized to 1. The upper left entry α can be eliminated by a skew linear transformation $\tilde{y}_1 = -\alpha x_2 + y_1$. Thus $\alpha = 0$ in (4.6), and henceforth. This proves that $A(0)$ indeed takes the form (3.8) with a Jordan block of order 3, generically.

Normal forms of vector fields with higher nilpotency have been studied extensively; see for example [CS86]. For the definitive exposition of normal forms, in general, see [Van89], [Tak73]. For our purposes we need a slight adaptation, restricting local transformations Φ of the vector field (4.1) to those near identity diffeomorphisms which map the equilibrium $\mathbf{y}$-plane $\mathbf{x} = 0$ into itself. We do not require Φ to fix this plane pointwise. In terms of Taylor polynomials, we successively expand

$$\Phi(z) \;=\; z + \Phi_2(z) + \cdots, \tag{4.7}$$

with $\Phi_k = (\Phi_k^{\mathrm{x}}, \Phi_k^{\mathrm{y}})$ homogeneous in z of degree k. The above restriction fixing the $\mathbf{y}$-plane $\mathbf{x} = 0$ amounts to

$$\Phi_k^{\mathrm{x}}(0, \mathbf{y}) \;=\; 0 \tag{4.8}$$

for all $\mathbf{y} \in \mathbb{R}^2$, $k = 2, 3, \ldots$.

In the Taylor expansion of the vector field $f(z) = Az + f_2(z) + \cdots$, transformations by Φ allows us to eliminate terms of f in the range of the Lie bracket $[\cdot, f]$,

$$[g, f](z) \;=\; g'(z)f(z) - f'(z)g(z), \tag{4.9}$$

up to any finite order k. Here g denotes the vector field which, as an element of the Lie algebra of the diffeomorphism group, generates the transformation Φ by the exponential map, i.e. by time integration of the vector field g. Expanding

$$g(z) \;=\; g_2(z) + \cdots \tag{4.10}$$

by order of z, we see that g enables us to successively eliminate components of $f_k(z)$ in the range of $\operatorname{ad} A$,

$$((\operatorname{ad} A)g)(z) \;=\; [A, g](z) \;=\; Ag(z) - g'(z)Az. \tag{4.11}$$

The normal form of f is then given, up to any finite order k, by a linear complement to the range of (4.11), as g is varied.

How do we keep track of the restriction (4.8) during this normal form process? Clearly the Lie algebra of associated vector fields $g = (g^{\mathrm{x}}, g^{\mathrm{y}})$ has to just satisfy

$$g_k^{\mathrm{x}}(0, \mathbf{y}) \;=\; 0 \tag{4.12}$$

for all $\mathbf{y} \in \mathbb{R}^2$, $k = 2, 3, \ldots$. The normal form of f then amounts to an element of the linear complement, in the space of vector fields f satisfying (4.2), to the range of $\operatorname{ad} A$ restricted to those g satisfying (4.12). Note here that $(\operatorname{ad} A)g$ satisfies (4.2) if g satisfies (4.12). Indeed, transformations by the flow of g preserve the $\mathbf{y}$-plane of equilibria of f,

and $A = A(0)$. The normal form itself depends on the choice of a complement in (4.11), (4.12), of course.

One of the many possible normal forms of f then takes the form

$$\begin{aligned}
\dot{x}_1 &= x_1 h_1(2x_1y_1 - x_2^2, \mathbf{y}) + x_2 h_2(2x_1y_1 - x_2^2, \mathbf{y}) + x_2^2 h_3(2x_1y_1 - x_2^2, \mathbf{y}),\\
\dot{x}_2 &= x_1,\\
\dot{y}_1 &= x_2,\\
\dot{y}_2 &= x_1 y_1 h_4(x_1y_1, \mathbf{y}),
\end{aligned} \tag{4.13}$$

with suitable formal Taylor series $h_1, \ldots, h_4$, up to any finite order. (Note the restriction $h_1(0,0) = h_2(0,0) = 0$ due to the prescribed linearization.) Indeed with $A = A(0)$ nilpotent as in (3.8), by (4.4)–(4.6) and g satisfying the restriction (4.12), we see that a complement to range(ad A) in the space of f satisfying (4.2) is spanned by $h_1, \ldots, h_4$ at any finite order k of g. Technical details of this calculation can be found in the appendix.

Truncating the general normal form (4.13) at second order, we obtain the same expression (4.13) with first-order terms $h_1 = h_{11}y_1 + h_{12}y_2$, $h_2 = h_{21}y_1 + h_{22}y_2$, and constants h_3, h_4:

$$\begin{aligned}
\dot{x}_1 &= x_1(h_{11}y_1 + h_{12}y_2) + x_2(h_{21}y_1 + h_{22}y_2) + h_3 x_2^2,\\
\dot{x}_2 &= x_1,\\
\dot{y}_1 &= x_2,\\
\dot{y}_2 &= h_4 x_1 y_1.
\end{aligned} \tag{4.14}$$

A linear transformation,

$$\begin{aligned}
\tilde{x}_1 &= -h_{21}x_1, \qquad & \tilde{y}_1 &= -h_{21}y_1 - h_{22}y_2,\\
\tilde{x}_2 &= -h_{21}x_2, \qquad & \tilde{y}_2 &= (h_{12}h_{21}/h_{11} - h_{22})y_2,
\end{aligned} \tag{4.15}$$

which will be motivated in sections 5–7 then converts (4.13) into the previously stated truncated normal form (3.9). We specifically note

$$a = h_{11}/h_{21}, \qquad b = -h_3/h_{11}, \tag{4.16}$$

and the nondegeneracy conditions

$$h_{11}, h_{21} \neq 0, \qquad h_{12}h_{21} - h_{11}h_{22} \neq 0. \tag{4.17}$$

5 Scaling, alias blow-up

Linearizing the normal form (3.9) at the $\mathbf{y}$-plane of equilibria, we obtain the unfolding

$$A(\mathbf{y}) = \begin{pmatrix} a(-y_1+y_2) & -y_1 & 0 & 0 \\ 1 & 0 & 0 & 0 \\ (c_1y_1+c_2y_2) & 1 & 0 & 0 \\ c_3(c_1y_1+c_2y_2) & 0 & 0 & 0 \end{pmatrix} \tag{5.1}$$

of the Jordan block or order 3 at $\mathbf{y}=0$. The analysis of the standard Takens-Bogdanov bifurcation crucially uses a scaling to near Hamiltonian form, which preserves the nilpotent Jordan block, of order 2 there, at $\lambda=0$. This is impossible, for nilpotencies of odd order. Instead, we present a scaling by small $0<\varepsilon<\varepsilon_0$ to near completely integrable form:

$$\begin{aligned} x_1 &= (\varepsilon/a)^4\tilde{x}_1, & y_1 &= (\varepsilon/a)^2\tilde{y}_1 \\ x_2 &= (\varepsilon/a)^3\tilde{x}_2, & y_2 &= (\varepsilon/a)^2\tilde{y}_2, \end{aligned} \tag{5.2}$$

and $t=a\varepsilon^{-1}\tilde{t}$. Inserting into the normal form (3.9) and omitting tildes, as well as terms of order ε^2 and beyond, we obtain

$$\begin{aligned} \dot{x}_1 &= -x_2y_1+\varepsilon(x_1(-y_1+y_2)+bx_2^2) \\ \dot{x}_2 &= x_1 \\ \dot{y}_1 &= x_2 \\ \dot{y}_2 &= 0 \end{aligned} \tag{5.3}$$

Note that y_2 has become simply a parameter in this scaling. Therefore the two viewpoints on Takens-Bogdanov bifurcation without parameters, as presented in section 3, (c) and the diversion (3.4), (3.5), coincide to order ε. To emphasize the foliation by $\dot{y}_2=0$, in the following sections, we will rename

$$\begin{aligned} \lambda &:= y_2 \\ y &:= y_1 \end{aligned} \tag{5.4}$$

and discuss the rescaled normal form

$$\begin{aligned} \dot{x}_1 &= -x_2y+\varepsilon(x_1(-y+\lambda)+bx_2^2) \\ \dot{x}_2 &= x_1 \\ \dot{y} &= x_2 \end{aligned} \tag{5.5}$$

for small $\varepsilon>0$. Understanding the solutions of (5.5) with

$$\|\mathbf{x}(t)\|,\ \|y(t)\|,\ |\lambda| \leq C, \tag{5.6}$$

for all $t\in\mathbb{R}$, and for $0\leq\varepsilon<\varepsilon_0(C)$, is a significant step towards understanding all solutions of the original system (1.3), (1.4) in a neighborhood $U\subset\mathbb{R}^4$ of the Takens-Bogdanov bifurcation at $z=(\mathbf{x},\mathbf{y})=0$. We therefore address system (5.5) in sections 6–9 below and return to the issue of omitted higher order terms in section 10.

6 Complete integrability, to scaling order zero

We consider the scaled vector field (5.5) to order zero in ε, that is

$$\begin{aligned} \dot{x}_1 &= -x_2 y \\ \dot{x}_2 &= x_1 \\ \dot{y} &= x_2. \end{aligned} \tag{6.1}$$

Equivalently, we rewrite (6.1) as a third order scalar equation

$$0 \;=\; \dddot{y} + y\dot{y} \;=\; \tfrac{\mathrm{d}}{\mathrm{d}t}(\ddot{y} + \tfrac{1}{2}y^2). \tag{6.2}$$

Immediately, this provides a first integral of motion

$$\Theta \;=\; \ddot{y} + \tfrac{1}{2}y^2 \;=\; x_1 + \tfrac{1}{2}y^2 \tag{6.3}$$

in terms of x_1, y. Considering (6.3) as a second order differential equation for y, on the other hand, we obtain the Hamiltonian system

$$\ddot{y} + \tfrac{1}{2}y^2 - \Theta \;=\; 0, \tag{6.4}$$

as was to be expected from a good Takens-Bogdanov type problem. The Hamiltonian provides a second integral of motion

$$H \;=\; \tfrac{1}{2}(\dot{y})^2 + \tfrac{1}{6}y^3 - \Theta y \;=\; \tfrac{1}{2}x_2^2 - x_1 y - \tfrac{1}{3}y^3. \tag{6.5}$$

Conversely, we can parametrize all trajectories of (6.1) by (Θ, H, y):

$$\begin{aligned} x_1 &= \Theta - \tfrac{1}{2}y^2 \\ x_2^2 &= -\tfrac{1}{12}q(y). \end{aligned} \tag{6.6}$$

Here $q(y)$ is the Weierstrass polynomial

$$q(y) \;=\; q(y; 24\Theta, 24H) \;=\; 4y^3 - 24\Theta y - 24H \tag{6.7}$$

with coefficients 24Θ and $24H$.

Before we perform a complete integration of (6.1) in terms of Weierstrass functions, in section 8, we record how to eliminate $\Theta > 0$ from (6.4) entirely by a simple scaling. Let $y(t) = y^{\Theta,H}(t)$ denote any solution of (6.4) with energy H. Then

$$y^{\Theta,H}(t) \;=\; \Theta^{1/2}\, y^{1,\tilde{H}}(\Theta^{1/4}t) \tag{6.8}$$

where $y^{1,\tilde{H}}$ is a solution of (6.4) with energy

$$\tilde{H} \;=\; \Theta^{-3/2}H. \tag{6.9}$$

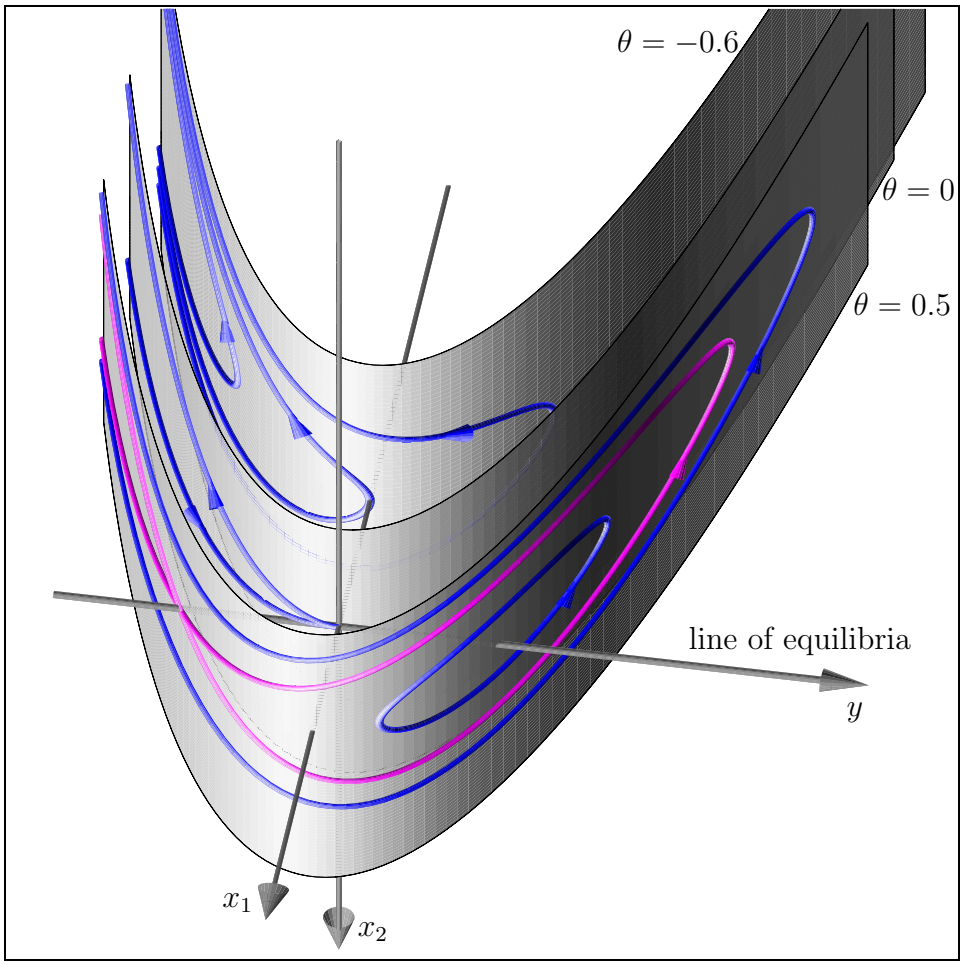

Figure 6.1: Phase portraits of the integrable scaled flow, at order zero in ε.

A similar scaling applies to the less interesting case $\Theta < 0$, where all orbits are unbounded.

With these remarks it is easy to plot the phase portraits of system (6.1); see figure 6.1. Note the x_2-independent invariant parabola sheets $x_1 = \Theta - \frac{1}{2}y^2$ which, for $\Theta \geq 0$, contain all bounded orbits. Also note how the collection of homoclinic orbits confines the set of bounded orbits. In fact, the homoclinic orbits emanate from the hyperbolic saddles, at $y < 0$, and loop around the positive y-axis before returning to the saddle. No further stationary orbits bifurcate from the equilibrium plane, represented by the y-axis. All remaining bounded orbits are periodic, forming a periodic "bubble".

Finally, we observe that the scaled flow is independent of the parameter $\lambda = y_2$, to order zero in ε. This absence of λ, which extremely facilitates the perturbation computations below and was already crucial to the simplicity of the scaling (6.8), (6.9), originated from our linear transformation (4.15) by which h_{22} was eliminated from our normal form (4.14).

7 Slow flow of first integrals, to order ε

With complete integrability at order ε^0 at hand, we now consider the scaled vector field (5.5) to order ε, that is

$$\begin{aligned} \dot{x}_1 &= -x_2 y + \varepsilon(x_1(-y+\lambda) + b x_2^2) \\ \dot{x}_2 &= x_1 \\ \dot{y} &= x_2. \end{aligned} \tag{7.1}$$

With $z = (x_1, x_2, y)$ and obvious notation for the scaled nonlinearities f_0, f_1, we abbreviate (7.1) as

$$\dot{z} = f_0(z) + \varepsilon f_1(z). \tag{7.2}$$

Parametrizing trajectories z by (Θ, H, y), according to (6.3), (6.5), (6.6), we obtain differential equations for Θ, H; for example

$$\dot{\Theta} = \Theta_z \cdot \dot{z} = \Theta_z f_0(z) + \varepsilon \Theta_z f_1(z), \tag{7.3}$$

where Θ_z indicates the gradient with respect to z. Note that $\Theta_z f_0(z) = 0$, because Θ is a first integral of the order zero flow; see section 6. We thus arrive at the slow flow for the first integrals

$$\begin{aligned} \dot{\Theta} &= \varepsilon \left[(\Theta - \tfrac{1}{2}y^2)(-y+\lambda) - \tfrac{1}{12} b q(y) \right] \\ \dot{H} &= -\varepsilon y \left[(\Theta - \tfrac{1}{2}y^2)(-y+\lambda) - \tfrac{1}{12} b q(y) \right]. \end{aligned} \tag{7.4}$$

In contrast to the slow motion of Θ, H, the variable y will move on a time scale of order one, for $\varepsilon \to 0$. Cutting through the bubble of periodic orbits, at order ε^0, we in fact have a Poincaré section Σ, transverse to the flow (7.1), defined by the half plane

$$\Sigma = \{(\mathbf{x}, y) \mid x_1 > 0 = x_2\}. \tag{7.5}$$

Indeed $\dot{x}_2 = x_1 > 0$ in Σ. The boundary of Σ consists of the equilibrium y-axis. A parametrization of Σ by (Θ, H) is given by choosing y as the middle one of the three solutions y of

$$q(y; 24\Theta, 24H) = 0 \tag{7.6}$$

and putting

$$x_1 := \Theta - \tfrac{1}{2}y^2. \tag{7.7}$$

The domain of definition of these coordinates is simply

$$\Theta^{-3/2}|H| = |\tilde{H}| < \tfrac{2}{3}\sqrt{2}, \qquad \Theta > 0. \tag{7.8}$$

The boundary of Σ is given by the values $\tilde{H} = \frac{2}{3}\sqrt{2}$, for the saddles at $y < 0$, and $\tilde{H} = -\frac{2}{3}\sqrt{2}$, for the foci at $y > 0$, with $y = 0$ relegated to $\Theta = 0$. This allows us to express the Poincaré return map

$$\Pi^\varepsilon \;:\; \Sigma \to \Sigma, \tag{7.9}$$

wherever defined, in terms of the coordinates (Θ, H) as $\Pi^\varepsilon(\Theta_0, H_0) = (\bar{\Theta}, \bar{H})$, where

$$\begin{aligned} \bar{\Theta} &= \Theta_0 + \int_0^{T^\varepsilon} \dot{\Theta}(t)\mathrm{d}t = \Theta_0 + \varepsilon I^\Theta(\varepsilon, \Theta_0, H_0) \\ \bar{H} &= H_0 + \int_0^{T^\varepsilon} \dot{H}(t)\mathrm{d}t = H_0 + \varepsilon I^{\mathrm{H}}(\varepsilon, \Theta_0, H_0). \end{aligned} \tag{7.10}$$

Here $T^\varepsilon = T^\varepsilon(\Theta_0, H_0)$ denotes the Poincaré return time.

The form (7.10) of the Poincaré return map Π^ε suggests to compute $I = (I^\Theta, I^{\mathrm{H}})$ at $\varepsilon = 0$ and to view Π^ε as a time discretization of first order, with time step ε, of the vector field

$$\frac{\mathrm{d}}{\mathrm{d}t}\begin{pmatrix}\Theta\\ H\end{pmatrix} = I(\Theta, H). \tag{7.11}$$

We call (7.11) the *Poincaré flow* of first integrals. The somewhat delicate issue of convergence of the integrals $I^\Theta(\varepsilon, \Theta_0, H_0)$, $I^{\mathrm{H}}(\varepsilon, \Theta_0, H_0)$ to their counterparts $I(\Theta_0, H_0)$, evaluated at $\varepsilon = 0$, is postponed to section 10.

By the form (7.4) of the (Θ, H)-flow, we then conclude

$$I(\Theta, H) = \int_0^{T^0} \left[(\Theta - \tfrac{1}{2}y^2)(-y + \lambda) - \tfrac{1}{12}bq(y)\right]\begin{pmatrix}1\\ -y\end{pmatrix}\mathrm{d}t. \tag{7.12}$$

Here $\varepsilon = 0$, and therefore Θ, H are fixed. The Poincaré time T^0 is the minimal period of the periodic orbit $y(t)$ of the integrable order zero vector field discussed in section 6. To evaluate the integrals (7.12) it is therefore sufficient to compute, for $k = 0, \ldots, 4$, the integrals

$$J_k = J_k(\Theta, H) = \int_0^{T^0} (y(t))^k \mathrm{d}t \tag{7.13}$$

for the periodic solution $y(t)$ of (6.4) which is determined by Θ, H. The simple scaling argument (6.8), (6.9) shows that

$$J_k(\Theta, H) = \Theta^{k/2-1/4} J_k(\tilde{H}), \tag{7.14}$$

where we have abbreviated $J_k(1, \tilde{H}) = J_k(\tilde{H})$. In the next section we recall a recursion relation and compute the complete elliptic integrals $J_k(\tilde{H})$ in terms of Weierstrass elliptic functions.

8 Elliptic integrals and Weierstrass functions

In this section we evaluate the complete elliptic integrals

$$J_k(\tilde{H}) \;:=\; \int_0^T (y(t))^k \mathrm{d}t, \tag{8.1}$$

for $k = 0, \ldots, 4$, as introduced in (7.13), (7.14), in terms of Weierstrass elliptic functions. We recall that $y(t) = y(t, \Theta = 1, H = \tilde{H})$ is a periodic solution of the second order equation (6.4), with $\Theta = 1$ and energy $H = \tilde{H}$, that is

$$\ddot{y} + \tfrac{1}{2}y^2 - 1 \;=\; 0 \tag{8.2}$$

$$\tfrac{1}{2}(\dot{y})^2 + \tfrac{1}{6}y^3 - y \;=\; \tilde{H}. \tag{8.3}$$

Note that $T = T(\tilde{H}) = J_0(\tilde{H})$ denotes the minimal period, for $|\tilde{H}| < \frac{2}{3}\sqrt{2}$. Also note the continuous limits

$$\begin{aligned} J_0(-\tfrac{2}{3}\sqrt{2}) &= 2^{3/4}\pi \\ J_0(\tfrac{2}{3}\sqrt{2}) &= +\infty \end{aligned} \tag{8.4}$$

corresponding to the Hamiltonian center at $y = \sqrt{2}$ and to the homoclinic saddle at $y = -\sqrt{2}$, respectively.

To establish the relation of $J_k(\tilde{H})$ to complete elliptic integrals, we recall

$$\dot{y}^2 \;=\; -\tfrac{1}{12}q(y) \tag{8.5}$$

from (6.5)–(6.7), where $q(y) = 4y^3 - 24y - 24\tilde{H}$ is the cubic Weierstrass polynomial. Following traditional notation, let $e_1 > e_2 > e_3$ denote the three real zeros of q depending on $\tilde{H} \in (-\frac{2}{3}\sqrt{2}, \frac{2}{3}\sqrt{2})$. Obviously then e_1, e_2 are the maximal, minimal values, respectively, of the periodic orbit $y(t)$. By time reversal symmetry these values occur at, say, $t = T/2$ and $t = 0$, respectively. We can therefore rewrite

$$J_k(\tilde{H}) \;=\; \int_0^T y(t)^k \mathrm{d}t \;=\; 2\int_{e_2}^{e_1} \frac{y^k}{\dot{y}} \mathrm{d}y \;=\; 2\int_{e_2}^{e_1} \frac{y^k}{\sqrt{-\frac{1}{12}q(y)}} \mathrm{d}y \tag{8.6}$$

which clearly identifies J_k as complete elliptic integrals.

Following an elementary exposition by [Tri37], [Tri48], we derive a two-term recursion for the elliptic integrals J_k. Just differentiate

$$\frac{\mathrm{d}}{\mathrm{d}y}\left(y^k\sqrt{q(y)}\right) \;=\; \frac{1}{\sqrt{q(y)}}\left(k y^{k-1} q(y) + \tfrac{1}{2}y^k q'(y)\right). \tag{8.7}$$

Integrating over y, from e_2 to e_1, and reinserting the factor $\sqrt{-1/12}$ indeed provides a linear 2-term recursion relation for J_k, because $q(e_j) = 0$. Therefore all J_k can be expressed linearly in terms of J_0 and J_1. For $k = 0, \ldots, 4$ we obtain explicitly

$$\begin{aligned} J_0 &= J_0(\tilde{H}) \\ J_1 &= J_1(\tilde{H}) \\ J_2 &= 2J_0 \\ J_3 &= \tfrac{6}{5}(3J_1 + 2\tilde{H}J_0) \\ J_4 &= \tfrac{12}{7}(2\tilde{H}J_1 + 5J_0). \end{aligned} \tag{8.8}$$

We now express J_0 in terms of the Weierstrass function $p(z)$, defined by the inverse elliptic integral

$$z + k\omega + \mathrm{i}l\omega' = \int^{p(z)} \frac{\mathrm{d}z}{\sqrt{q(z)}} \tag{8.9}$$

See for example [Tri48], [HC64] [Lan87] for some background. Due to the complex Riemann surface of $\sqrt{q(z)}$, two complex periods ω, $\mathrm{i}\omega'$ of the complex Weierstrass function $q(z)$ arise. Choosing $\omega, \omega' > 0$ we see that

$$J_0(\tilde{H}) = 2\sqrt{3}\omega'. \tag{8.10}$$

Indeed, $p(\omega/2) = e_1$, $p((\omega + \mathrm{i}\omega')/2) = e_2$, and (8.10) follows by multiplication with $\sqrt{-1/12}$ and $J_0, \omega' > 0$.

To compute J_1 we note that the definition (8.9) of the Weierstrass function $p(z)$ implies

$$y^{1,\tilde{H}}(t) = p(\sqrt{-1/12}\,(t + t_0)) \tag{8.11}$$

by separation of variables in (8.3). Therefore

$$\begin{aligned} J_1(\tilde{H}) &= \int_0^T y(t)\mathrm{d}t = \int_0^{J_0(\tilde{H})} y^{1,\tilde{H}}(t)\mathrm{d}t \\ &= \int_0^{\sqrt{12}\omega'} p(\sqrt{-1/12}\,t)\mathrm{d}t = -\sqrt{-12}\int_0^{\mathrm{i}\omega'} p(z)\mathrm{d}z \\ &= 2\sqrt{3}\,\mathrm{i}\,\zeta(\mathrm{i}\omega'), \end{aligned} \tag{8.12}$$

where $\zeta = -\int p$ denotes the Weierstrass ζ-function. The sign of the derived expression for J_1 can, in case of doubt, be derived by continuation from $\tilde{H} = -\frac{2}{3}\sqrt{2}$, where $\omega' = 2^{-1/4}3^{-1/2}\pi$ and $J_1 = 2^{5/4}\pi$.

For later reference we collect some further properties of J_0, J_1. It is possible to analytically show continuity at $\tilde{H} = \pm\frac{2}{3}\sqrt{2}$ of the following expressions

$$2J_1 + 3\tilde{H}J_0 = \begin{cases} 0 & \text{at } \tilde{H} = -\frac{2}{3}\sqrt{2} \\ 2^{13/4}\cdot 3 & \text{at } \tilde{H} = \frac{2}{3}\sqrt{2} \end{cases} \tag{8.13}$$

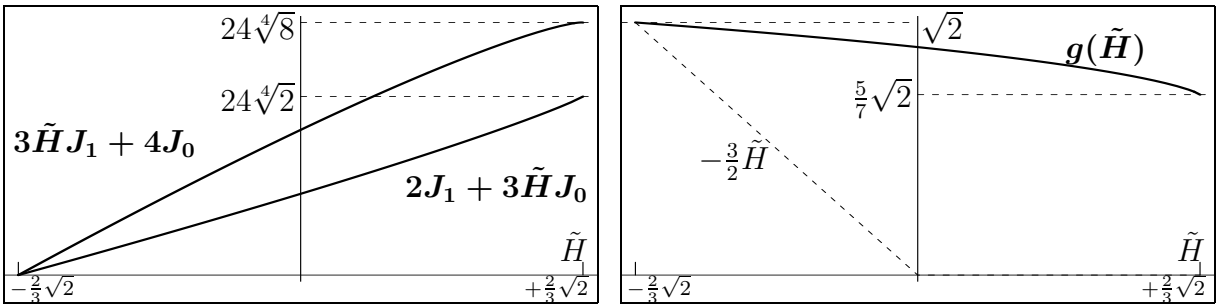

Figure 8.1: Plots of the nonlinearities $2J_1 + 3\tilde{H}J_0$, $3\tilde{H}J_1 + 4J_0$, and $g(\tilde{H})$.

Similarly, we obtain the limiting values of

$$3J_1\tilde{H} + 4J_0 \;=\; \begin{cases} 0 & \text{at } \tilde{H} = -\frac{2}{3}\sqrt{2} \\ 2^{15/4}\cdot 3 & \text{at } \tilde{H} = \frac{2}{3}\sqrt{2} \end{cases} . \tag{8.14}$$

Numerical inspection of the expressions (8.13), (8.14) by Mathematica indicates, but of course does not quite prove, positivity:

$$2J_1 + 3\tilde{H}J_0 \;>\; 0, \qquad\qquad 3\tilde{H}J_1 + 4J_0 \;>\; 0 \tag{8.15}$$

for $-\frac{2}{3}\sqrt{2} < \tilde{H} \leq \frac{2}{3}\sqrt{2}$. Concerning the quotient nonlinearity

$$g(\tilde{H}) \;:=\; \frac{5}{7}\,\frac{3\tilde{H}J_1 + 4J_0}{2J_1 + 3\tilde{H}J_0} \tag{8.16}$$

which will play a crucial role in section 9, we note the limiting values

$$g(\tilde{H}) \;=\; \begin{cases} \sqrt{2} & \text{at } \tilde{H} = -\frac{2}{3}\sqrt{2} \\ \frac{5}{7}\sqrt{2} & \text{at } \tilde{H} = \frac{2}{3}\sqrt{2} \end{cases} . \tag{8.17}$$

The limit at $\tilde{H} = \frac{2}{3}\sqrt{2}$ follows from (8.13), (8.14). The limit at $\tilde{H} = -\frac{2}{3}\sqrt{2}$ follows easily when relating $g(\tilde{H})$ back to the change of stability along the Hopf line $\lambda = y$ in the equilibrium plane; see (9.10). We will also trust the numerics of Mathematica to reliably indicate that

$$\tfrac{5}{7}\sqrt{2} \;<\; g(\tilde{H}) \;<\; \sqrt{2}, \qquad\qquad -\tfrac{3}{2}\tilde{H} \;<\; g(\tilde{H}) \tag{8.18}$$

for $|\tilde{H}| < \frac{2}{3}\sqrt{2}$, see figure 8.1.

9 Poincaré flows of first integrals

Further postponing the issue of higher order perturbations slightly, we study the Poincaré flow (7.11), in this section. By (7.12)–(7.14) and recursions (8.8) for the complete elliptic integrals $J_k(\tilde H)$, the Poincaré flow takes the form

$$\begin{aligned}\dot\Theta &= \tfrac{2}{5}\Theta^{5/4}(b+1)(2J_1+3\tilde H J_0)\\ \dot H &= 2\Theta^{7/4}\left(\tfrac{1}{5}\lambda\Theta^{-1/2}(2J_1+3\tilde H J_0)-\tfrac{1}{7}(b+2)(3\tilde H J_1+4J_0)\right)\end{aligned} \tag{9.1}$$

Here $J_0=J_0(\tilde H)$, $J_1=J_1(\tilde H)$ as in section 8. To derive (9.1) we evaluate the integrals $I(\Theta,H)$ in (7.12) along $y(t)=y^{\Theta,H}(t)$, then substitute $y^{1,\tilde H}$ by (6.8), replace H by $\tilde H=\Theta^{-3/2}H$ according to (6.9), and apply recursions (8.8) which only hold for $\Theta=1$, before grouping terms as in (9.1). Since $J_k=J_k(\tilde H)$ we prefer to use $\tilde H$ as a variable in (9.1) directly and write

$$\begin{aligned}\dot\Theta &= \tfrac{2}{5}\Theta^{5/4}(b+1)(2J_1+3\tilde H J_0)\\ \dot{\tilde H} &= \tfrac{2}{5}\Theta^{1/4}(b+1)(2J_1+3\tilde H J_0)\left(\tfrac{\lambda}{b+1}\Theta^{-1/2}-\tfrac{3}{2}\tilde H-\alpha g(\tilde H)\right)\end{aligned} \tag{9.2}$$

where we have abbreviated

$$\begin{aligned}\alpha &= \frac{b+2}{b+1} = 1+\frac{1}{b+1}\\ g(\tilde H) &= \frac{5}{7}\,\frac{3\tilde H J_1(\tilde H)+4J_0(\tilde H)}{2J_1(\tilde H)+3\tilde H J_0(\tilde H)}\end{aligned} \tag{9.3}$$

We recall the properties of the right-hand sides of the Poincaré-flow (9.2) as collected in section 8, (8.13)–(8.18). We have assumed $b\neq -1$ so that $b+1\neq 0$. Moreover $\Theta>0$ is invariant, and $2J_1+3\tilde H J_0>0$ except for the centers $\tilde H=-\frac{2}{3}\sqrt{2}$. Therefore it makes sense to parametrize all $(\Theta,\tilde H)$-orbits over $\tau=\log\Theta$. Writing $'=\frac{d}{d\tau}$ this leads to the simplified equation

$$\tilde H'(\tau) = \tfrac{\lambda}{b+1}\mathrm{e}^{-\tau/2}-\tfrac{3}{2}\tilde H-\alpha g(\tilde H). \tag{9.4}$$

It is obvious that we can now absorb the value $|\lambda/(b+1)|$ into a mere shift of "time" τ, as long as $\lambda=y_2\neq 0$. The autonomous case $\lambda=0$ corresponds to the limiting case $\tau=+\infty$ discussed below and will be omitted for its simplicity. To understand the dynamics of the Poincaré flow (7.11) for $\lambda\neq 0$, it is therefore sufficient to discuss the two vector fields

$$\tilde H'(\tau) = \pm\mathrm{e}^{-\tau/2}-\tfrac{3}{2}\tilde H-\alpha g(\tilde H) \tag{9.5}$$

for the various regimes of the real parameter $\alpha=1+1/(b+1)$. For each of the signs $\pm$

which is given by $\mathrm{sign}(\lambda(b+1))$, the following three cases arise

$$\begin{array}{lrcl} \text{Case (A)} & b<-17/12 & \Longleftrightarrow & -7/5<\alpha<1 \\ \text{Case (B)} & -17/12<b<-1 & \Longleftrightarrow & \alpha<-7/5 \\ \text{Case (C)} & -1<b & \Longleftrightarrow & 1<\alpha \end{array} \tag{9.6}$$

Phase portraits of the six resulting cases are provided in figure 9.1.

We comment on the derivation and interpretation of these phase portraits next. First we recall that orbits of (9.2) and (9.5) coincide, if we put

$$\Theta \;=\; (\tfrac{\lambda}{b+1})^2 \mathrm{e}^{\tau}. \tag{9.7}$$

For $b<-1$ however, the time direction of (9.5) has to be reversed to account for the time direction vested into these orbits by (9.2).

We also recall that $\tilde H = -\frac{2}{3}\sqrt{2}$ refers to the equilibrium half line $\mathbf{x}=0$, $y_1 = y = \sqrt{2\Theta} > 0$, for any $y_2 = \lambda$, in terms of the original Takens-Bogdanov system (3.1)–(3.3), (3.6), (3.7) and its normal forms (3.9), (4.13), (5.3), (5.5); see also figure 3.1. Indeed $\Theta^{-3/2} H = \tilde H = -\frac{2}{3}\sqrt{2}$, $y = \sqrt{2\Theta}$, and the definitions (6.3), (6.5)–(6.7) of Θ, H imply $\mathbf{x}=0$, $y>0$. Consistently with this observation, both $\dot\Theta$ and $\dot{\tilde H}$ vanish along this line, because $2J_1 + 3\tilde H J_0 = 0$ at $\tilde H = -\frac{2}{3}\sqrt{2}$; see (8.13). In the original coordinates $(\mathbf{x}, y)$ these equilibria are normally hyperbolic, except along the Hopf line

$$\lambda \;=\; y \;>\; 0. \tag{9.8}$$

Indeed, the (strict) unstable dimension is 2, for $0<y<\lambda$, and 0 for $0<\lambda<y$. These unstable dimensions are easily detected in the right half of figure 9.1.

In the $(\tilde H, \tau)$-coordinates of (9.4), the Hopf line (9.8) manifests itself by a horizontal tangent

$$\tilde H' \;=\; 0. \tag{9.9}$$

at $\tilde H = -\frac{2}{3}\sqrt{2}$, for any fixed $\lambda > 0$. Evaluating condition (9.9) together with $\lambda = y = \sqrt{2\Theta}$ immediately yields the limiting value

$$g(-\tfrac{2}{3}\sqrt{2}) \;=\; \sqrt{2} \tag{9.10}$$

as was claimed in (8.17). For fixed $\lambda<0$, in the left half of figure 9.1, we just as easily detect strict normal stability of the equilibria $\mathbf{x}=0$, $y>0$.

For very negative τ, alias small $\Theta>0$, it is easy to discuss the orbits of (9.5). Since $|\tilde H| \le \frac{2}{3}\sqrt{2}$ and $\frac{5}{7}\sqrt{2} \le g \le \sqrt{2}$ are uniformly bounded in the region of interest, we obtain

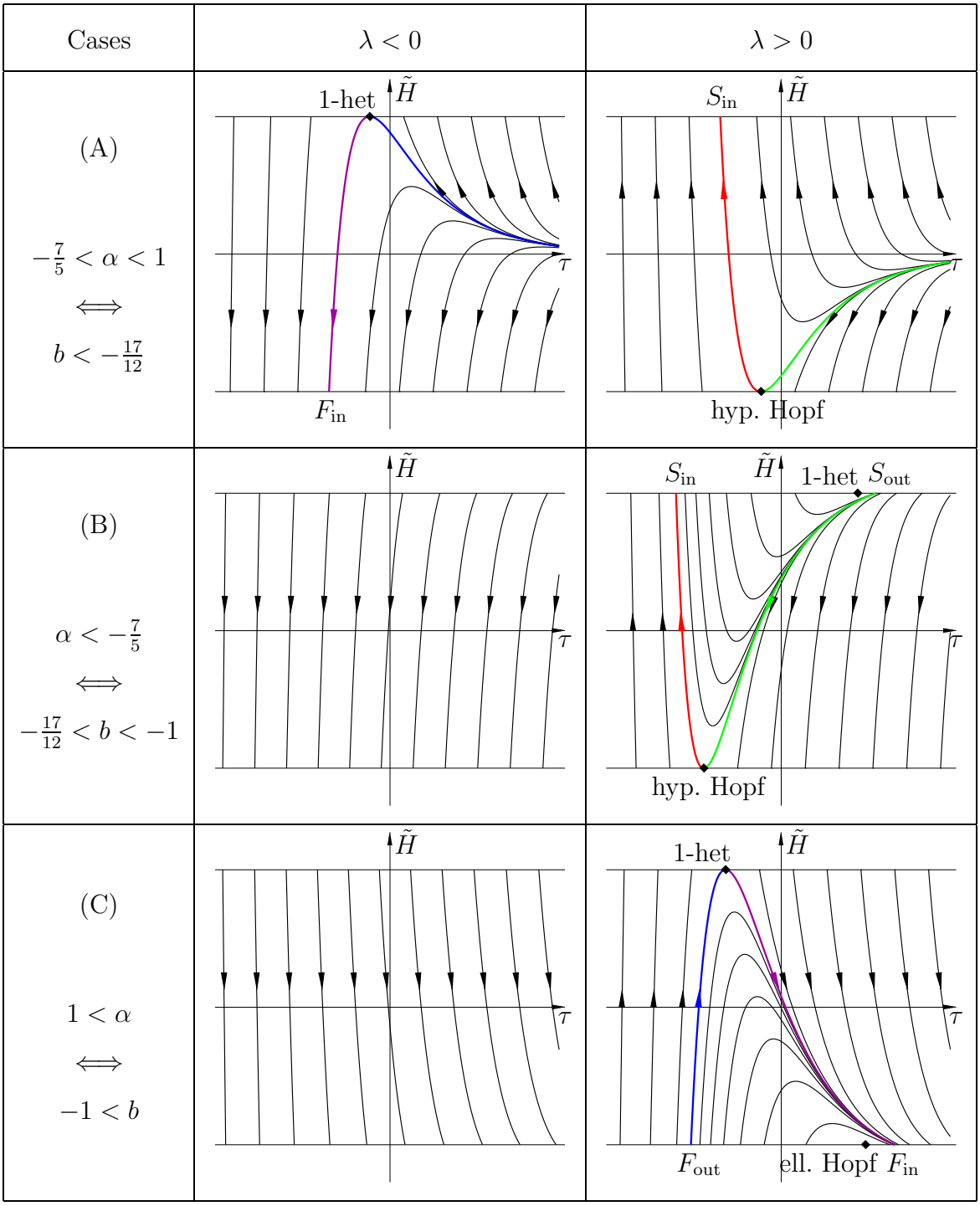

Figure 9.1: Phase portraits of equation (9.5), see also (9.3), (9.6) and the explanations following there. Time direction refers to the flow (9.2).

almost vertical orbits which connect the horizontal boundaries $\tilde{H} = \pm\frac{2}{3}\sqrt{2}$ in very short "time" intervals τ. The direction, with proper reversal for $b < -1$, is easily determined.

For very positive τ, as well as for $\lambda = 0$, the exponential term disappears and we are left with the autonomous limiting equation

$$-\tilde{H}'(\tau) \;=\; \tfrac{3}{2}\tilde{H} + \alpha g(\tilde{H}). \tag{9.11}$$

We use properties (8.17), (8.18) of g to study this limiting equation for $|\tilde{H}| < \frac{2}{3}\sqrt{2}$. Since $\frac{5}{7}\sqrt{2} \le g \le \sqrt{2}$ and $-\frac{3}{2}\tilde{H} \le g$, the right-hand side possesses zeros if, and only if,

$$-\tfrac{7}{5} \;<\; \alpha \;<\; 1. \tag{9.12}$$

Only in this case (A), therefore, the orbits of (9.5) do not connect the horizontal boundaries $\tilde{H} = \pm\frac{2}{3}\sqrt{2}$ within finite "time" τ, for all large positive τ, as they did for very negative τ and still do for large positive τ in the other cases (B), (C). Rather, in case (A), the zero or, hypothetically, zeros of $\frac{3}{2}\tilde{H} + \alpha g(\tilde{H})$ provide semi-invariant regions, for large $\tau > 0$, which prevent orbits from connecting the horizontal boundaries. Instead,

$$\lim_{\tau\to+\infty} \tilde{H}(\tau) \;\in\; (-\tfrac{2}{3}\sqrt{2}, +\tfrac{2}{3}\sqrt{2}) \tag{9.13}$$

exists for all orbits starting at sufficiently large $\tau > 0$. This accounts for the shaded regions labeled "y-entry", in figure 3.1 (A). Note that the backwards escape time $t < 0$ is finite in terms of the original system (9.1), due to (9.13) and positivity property (8.15) of $2J_1 + 3\tilde{H}J_0$.

We discuss the upper horizontal boundary $\tilde{H} = +\frac{2}{3}\sqrt{2}$ next. This $\tilde{H}$-value does not only indicate the half line of saddle equilibria $\mathbf{x} = 0$, $y = -\sqrt{2\Theta} < 0$, which can be discussed analogously to the case $\tilde{H} = -\frac{2}{3}\sqrt{2}$ treated above. It also characterizes the fate under perturbation to positive ε of the family of homoclinic orbits, which exists for $\varepsilon = 0$. This latter view point is in fact the only appropriate one, if we insert the nonzero limiting values (8.13), (8.14), (8.17) in (9.1), (9.5), at $\tilde{H} = \frac{2}{3}\sqrt{2}$. Then $\dot{\Theta} \neq 0$ along this line, and $\tilde{H}'$ vanished only at the simple zero

$$\pm e^{-\tau/2} \;=\; (\tfrac{3}{2}\tilde{H} + \alpha g(\tilde{H})) \;=\; \sqrt{2}\frac{12b+17}{7(b+1)} \tag{9.14}$$

of the right hand side of (9.5). In terms of (9.2) and the original (scaled) variables $y = -\sqrt{2\Theta} = \mp\sqrt{2}e^{\tau/2}\lambda/(b+1)$ this occurs along the asymptote

$$\lambda \;=\; -\tfrac{1}{7}(12b+17)y. \tag{9.15}$$

These points in figure 9.1, and lines in figure 3.1, are labeled "1-het". They correspond to zeros of an associated Melnikov function and to saddle-saddle heteroclinic orbits, in the

original system, as we will see in the next section. The remaining boundary regions $\tilde{H} = \frac{2}{3}\sqrt{2}$ where $\dot{\tilde{H}}$ is positive or negative, respectively, indicate a splitting of the homoclinic bubble such that orbits escape in backward or forward time from a neighborhood U of the origin in the equilibrium plane $\mathbf{x} = 0$. In figure 3.1 this behaviour is marked as "x-entry/exit".

10 Higher order: Poincaré flow, averaging, Melnikov

Before completing our analysis of Takens-Bogdanov bifurcations without parameters, in section 11, we now digress for a discussion of the effects of omitted higher order terms. We recall the three approximation steps which we have applied:

(a) truncation to second order normal form (section 4)

(b) omission of scaling terms of order ε^2 and higher (section 5)

(c) approximation of the Poincaré map Π^ε by the time ε map of the Poincaré flow (section 7, (7.9)–(7.12)).

To ensure that our original variables $((\varepsilon/a)^4 x_1, (\varepsilon/a)^3 x_2, (\varepsilon/a)^2 y, (\varepsilon/a)^2 \lambda)$ cover a neighborhood U of the origin in $\mathbb{R}^4$, we fix $C > 0$ arbitrarily large, consider the scaled variables (x_1, x_2, y, λ) in a ball of radius C, and analyze the complete, non-truncated rescaled dynamics for $0 \leq \varepsilon < \varepsilon_0 = \varepsilon_0(C)$.

In terms of the variables $(\tau, \tilde{H}, y)$, $\tau = \log \Theta$, we immediately see that solutions which do not intersect the Poincaré section

$$\Sigma \;=\; \{(\tau, \tilde{H}, y) \mid \tau \in \mathbb{R},\ |\tilde{H}| < \tfrac{2}{3}\sqrt{2},\ y = e_2\} \tag{10.1}$$

become unbounded, or else belong to some equilibrium in the closure $\bar{\Sigma}$ or to its strong stable or strong unstable manifold $W^{\mathrm{ss}}(y)$, $W^{\mathrm{uu}}(y)$. As before $e_2 = e_2(\Theta, H)$ denotes the middle zero of the Weierstrass polynomial $q(y)$, where indeed $x_2 = 0$; see (6.6), (6.7), figure 6.1, and (7.6), (8.6).

We are interested in bounded nonstationary solutions which remain in U and thus intersect Σ. We have seen in section 7, that the Poincaré map Π^ε, wherever defined on Σ, is just some first order discretization of the Poincaré flow (7.11), (7.12) with time step ε. This statement concerning approximation (c) was made for Poincaré maps Π^ε which arise after completion of the approximation steps (a), (b). More generally, we observe that the same statement evidently remains true, when approximations (a), (b) are included. Indeed, we then include the "parameter" $\lambda = y_2$ into our construction of Σ, Π^ε, and the

Poincaré flow. Since the omitted terms perturb the Poincaré map Π^ε, by terms of order ε^2 *or higher* order, the map Π^ε remains a first order discretization of the *unperturbed* Poincaré flow.

In the remainder of this section we discuss two issues. First, we recall how the Poincaré flow and its discretization Π^ε relate to the usual averaging approach. Second, we relate the Poincaré flow and Π^ε to the Melnikov functions associated to the family of homoclinic orbits. In particular we address the behavior of Π^ε near the saddle boundary $\tilde{H} = \frac{2}{3}\sqrt{2}$ of the Poincaré section Σ.

The averaging procedure aims at eliminating the oscillations of y from the slow flow of (Θ, H) in (7.4). See [BM61], [Hal63], [Arn83] for a background. The elimination is achieved by successive y-dependent transformations of (Θ, H). These transformations successively lead to autonomous vector fields for (Θ, H), independent of y, with y-dependent corrections of order ε^N, $N = 2, 3, \ldots$. The first step $N = 2$ replaces y^k in (7.4) by the time average

$$\frac{1}{T}\int_0^T (y(t))^k \mathrm{d}t \;=\; \frac{J_k}{J_0}, \tag{10.2}$$

over the unperturbed T-periodic solution $y(t)$, in the notation of (7.13). Replacing J_k by J_k/J_0, everywhere, converts our Poincaré flow (7.11), (7.12) to the first averaged flow of the standard approach. The Poincaré flow and the averaged flow just differ by an Euler multiplier $T = T(\Theta, H) = J_0$. In particular the analysis of section 9 applies. Except for our interpretation of the Poincaré map Π^ε as the time ε discretization, rather than a time $T \cdot \varepsilon$ discretization, of the (Θ, H) flow the two view points are completely equivalent — as long as $T(\Theta, H) = J_0$ remains finite.

Near homoclinicity, alias near $J_0 = \infty$ or near the upper horizontal boundary $\tilde{H} = \frac{2}{3}\sqrt{2}$, the Poincaré flow (7.11), (7.12) offers an advantage, because the vector field $I = I(\Theta, H)$ can be interpreted directly in terms of Melnikov functions. See [CH82], [FS96] for a background. For systems

$$\dot{z} \;=\; f_0(z) + \varepsilon f_1(\varepsilon, z) \tag{10.3}$$

with an unperturbed homoclinic orbit $z(t)$, at $\varepsilon = 0$, a Melnikov function M associated to $z(t)$ is given by

$$M \;=\; \int_{-\infty}^{+\infty} \psi(t)^T f_1(0, z(t)) \mathrm{d}t, \tag{10.4}$$

where ψ is a nontrivial bounded solution of the adjoint variational equation

$$\dot{\psi} \;=\; -(\mathrm{D_z} f_0(z(t)))^T \psi. \tag{10.5}$$

In the presence of first integrals Θ, H at $\varepsilon = 0$ we may choose

$$\psi(t) \;=\; \mathrm{D_z}\Theta(z(t)),\ \mathrm{D_z}H(z(t)) \tag{10.6}$$

and obtain corresponding Melnikov functions $M^\Theta, M^{\rm H}$. By definition (7.11), (7.12), these Melnikov functions coincide with the components of the Poincaré flow $I = (I^\Theta, I^{\rm H})$:

$$M^\Theta \;=\; I^\Theta, \qquad M^{\rm H} \;=\; I^{\rm H} \tag{10.7}$$

at homoclinic orbits.

As in classical Melnikov theory, which usually deals with nondegenerate homoclinic orbits rather than families of homoclinic orbits, the terms $\pm\varepsilon(I^\Theta, I^{\rm H})(\Theta_0, H_0)$ indicate the leading order in ε of the return to Σ of the strong unstable and strong stable manifolds $W^{\rm uu}(y)$, $W^{\rm ss}(y)$, respectively, of the saddle equilibrium at $y = -\sqrt{2\Theta_0}$, $\Theta_0^{-3/2} H_0 = \tilde H = \frac{2}{3}\sqrt{2}$. This of course assumes that the corresponding point

$$\begin{aligned} \hat\Theta \;&=\; \Theta_0 \pm \varepsilon I^\Theta(\Theta_0, H_0) \\ \hat H \;&=\; H_0 \pm \varepsilon I^{\rm H}(\Theta_0, H_0) \end{aligned} \tag{10.8}$$

actually lies in Σ, to within order ε^2. Similarly, orbits for which $(\hat\Theta, \hat H)$ lies outside Σ, to within order ε, do not return. Indeed the integrals $I = (I^\Theta, I^{\rm H})(\varepsilon, \Theta_0, H_0)$ in (7.10) converge of order ε, uniformly for $T^\varepsilon \leq \infty$, as long as the orbit starting at $(\Theta_0, H_0) \in \bar\Sigma$ does return to Σ. For saddle equilibria $(\Theta_0, H_0) \in \partial\Sigma$ where $T^\varepsilon = +\infty$, we only have to replace the return point $(\bar\Theta, \bar H)$ in Σ by the return point of the strong unstable or strong stable manifold of (Θ_0, H_0) and observe the uniform estimate

$$\|(\bar\Theta, \bar H) - (\hat\Theta, \hat H)\| \;=\; \mathcal{O}(\varepsilon^2). \tag{10.9}$$

In section 9 we have determined "heteroclinic" values of $\Theta_0 > 0$ for which

$$\dot{\tilde H} \;=\; 0 \tag{10.10}$$

at the saddle boundary $\tilde H = \frac{2}{3}$; see (9.14), (9.15). Because these zeros of $\dot{\tilde H}$ are simple, with respect to Θ, an adaptation of standard Melnikov theory shows the existence of nearby heteroclinic orbits. To within order ε^2, these orbits start at the computed values of Θ_0, $H_0 = \frac{2}{3}\sqrt{2}\Theta_0^{3/2}$, y, λ and terminate at the value $\hat y$, λ associated to $\hat\Theta$, $\hat H = \frac{2}{3}\sqrt{2}\hat\Theta^{3/2}$. By (10.8), (9.15) the corresponding values y, $\hat y$ differ by order $\varepsilon\lambda$. In terms of the original variables $y_1 = (\varepsilon/a)^2 y$, $y_2 = (\varepsilon/a)^2\lambda$ we therefore obtain a cusp of saddles in the equilibrium $\mathbf{y}$-plane, with the two half-arcs connected almost horizontally by a heteroclinic orbit. Indeed the horizontal width of the heteroclinic sector is of order ε^3 at distance ε^2 from the origin.

11 Geometry of Poincaré maps

In this section we complete our analysis of Takens-Bogdanov bifurcations without parameters. In particular we complete our proof of the heteroclinic and x-entry/exit orbits indicated in figure 3.1. Although higher order terms introduce a small drift in the "parameter" λ, we may safely ignore this effect for simplicity of presentation. Likewise, we omit a discussion of the rather simple case $\lambda = 0$ for brevity.

In the previous section we have advocated to use the (Θ, H) Poincaré flow (9.1) not only on the Poincaré section Σ given by $|\tilde{H}| < \frac{2}{3}\sqrt{2}$, $\tau \in \mathbb{R}$, but up to the boundary $\tilde{H} = \frac{2}{3}\sqrt{2}$ of the saddle equilibria $y < 0$ and their strong stable and unstable manifolds $W^{\rm ss}(y)$, $W^{\rm uu}(y)$. Alternatively to (Θ, H), we can use the coordinates $\tau = \log(\Theta((b+1)/\lambda)^2)$, $\tilde{H} = \Theta^{-3/2}H$ of (9.5) and figure 9.1. Note, however, that a time ε discretization step of (9.1) as realized by the Poincaré return map Π^ε corresponds to a τ-step of size

$$\Theta^{-1}\dot{\Theta}\varepsilon \;\; = \;\; \tfrac{2}{5}\Theta^{1/4}(b+1)(2J_1 + 3\tilde{H}J_0)\cdot\varepsilon \tag{11.1}$$

Near the saddle boundary where Melnikov theory applies this expression simplifies to a τ-step of

$$\Theta^{-1}\dot{\Theta}\varepsilon \;\; = \;\; \tfrac{48}{5}(2\Theta)^{1/4}(b+1)\cdot\varepsilon, \tag{11.2}$$

by (8.13). As was pointed out earlier, we may restrict our analysis to regions $|\tilde{H}| \le \frac{2}{3}\sqrt{2}$, $\tau \le C$, and $0 < \varepsilon < \varepsilon_0(C)$.

We first consider the simplest cases: $(B), (C)$ with $\lambda < 0$. In these two cases all orbits of the Poincaré flow are pointing strictly downwards. Therefore, the collection

$$W^{\rm cu} \;\; = \;\; \bigcup_{y<0} W^{\rm uu}(y) \tag{11.3}$$

of strong unstable manifolds of the saddles intersects Σ in an infinite sequence of "horizontal" lines, accumulating to the stable equilibria along $\tilde{H} = -\frac{2}{3}\sqrt{2}$. All points of Σ in between these lines leave the neighborhood U of $\mathbf{x} = \mathbf{y} = 0$, in backwards time, while converging to the stable equilibria in forward time. We can view $W^{\rm cu}$ as a two-dimensional scroll, forward spiraling into the equilibria $\mathbf{x} = 0$, $y > 0$. It is an interesting warm-up to visualize this scroll in figure 6.1.

The two most interesting cases are cases (B) and (C) with $\lambda > 0$ which exhibit Hopf bifurcation, without parameters of course, in coexistence with saddle heteroclinic orbits $\dot{\tilde{H}} = 0$ at $\tilde{H} = \frac{2}{3}\sqrt{2}$ as discussed in section 10. The remaining two moderately interesting cases, (A) with $\lambda > 0$ and $\lambda < 0$, are similar to cases (B) and (C) with $\lambda > 0$, respectively: the former preserves the hyperbolic Hopf point but the heteroclinic orbit has disappeared

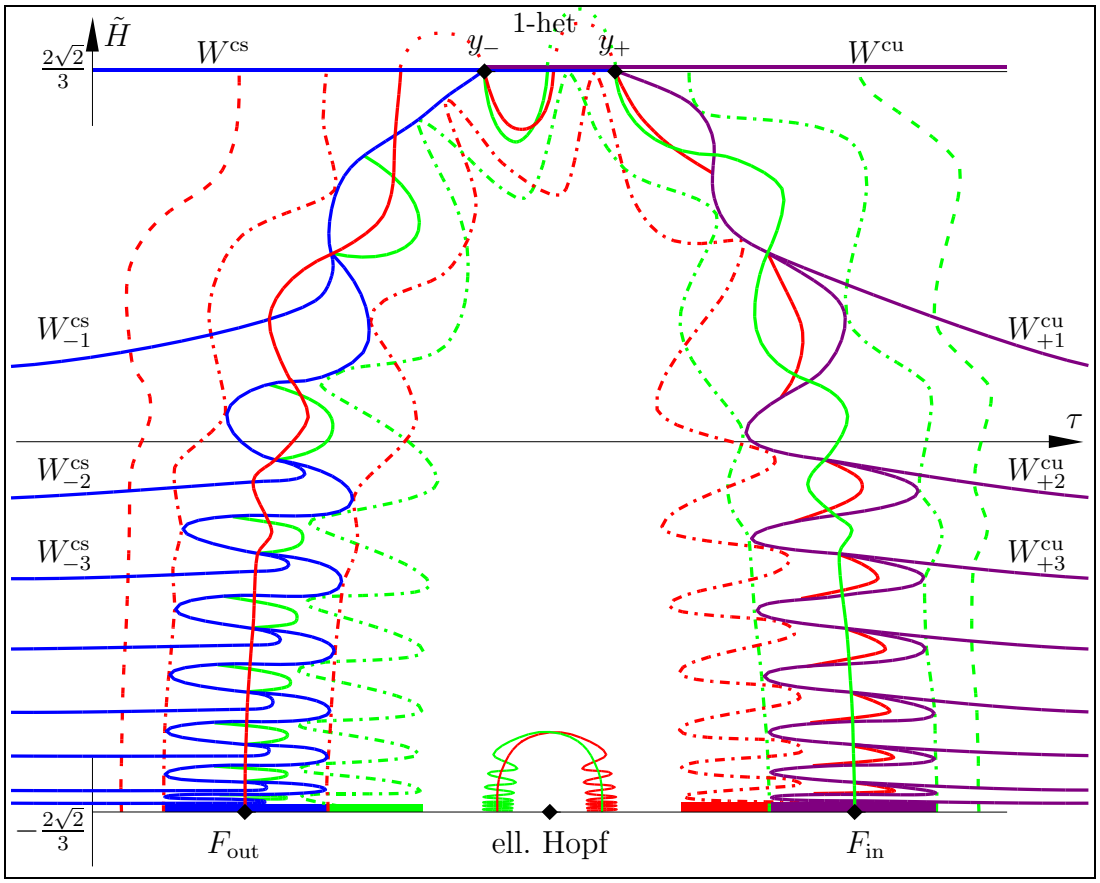

Figure 11.1: Poincaré section Σ of case (C), $\lambda > 0$ of figure 9.1. Coding: magenta = W^{cu}(saddle), blue = W^{cs}(saddle), red = W^{uu}(center), and green = W^{ss}(center).

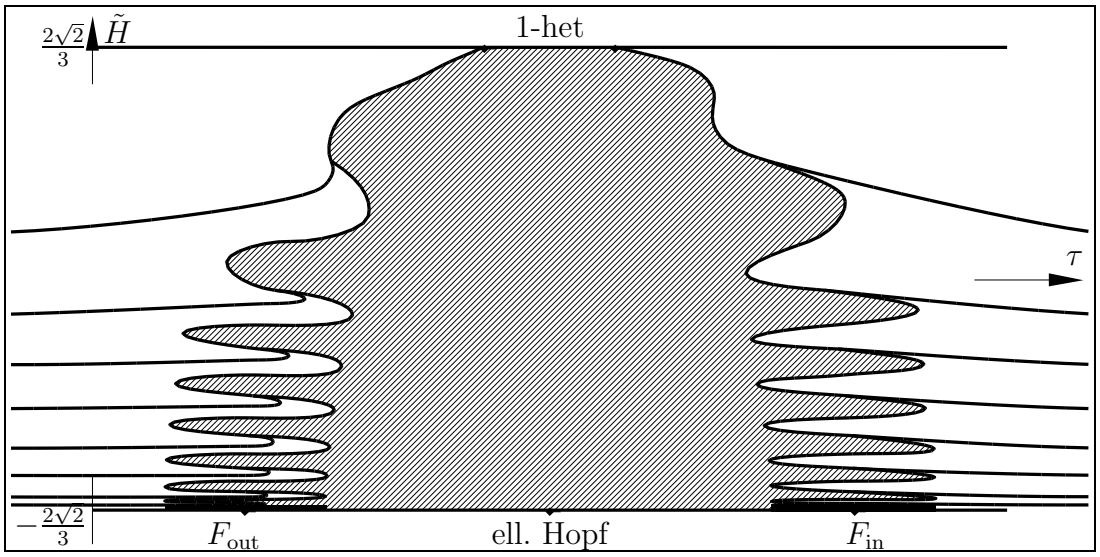

Figure 11.2: Set of bounded orbits in the Poincaré section Σ of case (C), $\lambda > 0$.

through $\tau = +\infty$. Conversely, the latter preserves that heteroclinic orbit but has pushed the elliptic Hopf point out through $\tau = +\infty$.

We first discuss the interesting case (C), $\lambda > 0$ which involves both a saddle heteroclinic orbit and an elliptic Hopf point; see figure 11.1. For a local section near the elliptic Hopf point which involves exponentially small splittings of heteroclinic separatrices see [FLA00a] and figure 2.3 (b) left. We first follow the saddle segment S, between the two saddle end points $y_\pm < 0$ of the saddle-saddle heteroclinic, forward under Π^ε. The (magenta) forward continuation is a piecewise smooth curve $W^{\rm c}_+$ with tangent jumps of order ε at the (forward) points $y_{+,n}$, $n = 0, 1, 2, \ldots$ of $W^{\rm uu}(y_+) \cap \Sigma$. Let

$$F_{\rm in} \;:=\; \lim_{n\to\infty} y_{+,n}$$

Typically the (green) curve $W^{\rm ss}(F_{\rm in})$ will intersect $W^{\rm c}_+$ transversely, even at the points $y_{+,n}$. The curve $W^{\rm c}_+$ will therefore limit to an interval of stable equilibria $y^{\rm c}_+ > 0$, around $F_{\rm in}$ to the right of the Hopf point. Note however, that transversality has not been proved but can typically be expected to hold for a first-order time ε discretization of the Poincaré flow as given, for example, by the Poincaré map Π^ε. Similar statements hold true for the (blue) backwards continuation $W^{\rm c}_-$ of S in Σ and its intersection with the (red) unstable manifolds $W^{\rm uu}(y^{\rm c}_-)$. We also illustrate the behavior of some strong stable and strong unstable manifolds of other equilibria $y > 0$ on the bottom line $\tilde H = -\frac{2}{3}\sqrt{2}$. Note how these manifolds transversely connect to equilibrium intervals on the other side of the elliptic Hopf point, or disappear partially, or disappear completely as their source points $y > 0$ move away from the Hopf point through $F_{\rm out}$. Also, transverse splitting effects should not be expected to be exponentially small any more, during this transition, but to be of order ε. Outside the "Hopf bubble" depicted in figure 11.2, we will encounter "horizontal" copies of the center manifolds $W^{\rm cu} \cap \Sigma$, $W^{\rm cs} \cap \Sigma$ of the saddles to the right, left, respectively, as we have indicated. These extend from the intersection points $y_{\pm,n}$ and form smooth continuations of the piece of $W^{\rm c}_\pm$ immediately above $y_{\pm,n}$. Again we note that all orbits are heteroclinic, as indicated in figure 3.1, with only one saddle-saddle heteroclinic, or also become unbounded through the split homoclinic family. These facts persist under higher order perturbations.

We now turn to the final interesting case (B), $\lambda > 0$, which involves both a saddle heteroclinic orbit and a hyperbolic Hopf point; see figure 11.3. For a local section near the hyperbolic Hopf point see again [FLA00a] and figure 2.3 (b) right. This local analysis shows that the Hopf point itself possesses a stable (and an unstable) half-arc $W^{\rm s}_{\rm Hopf}$, ($W^{\rm u}_{\rm Hopf}$) indicated in green (red) and terminating at saddle points $S_{\rm out}$, $S_{\rm in}$ to the right (left) of the Hopf point. We encounter the strong stable (unstable) manifolds of the equilibria $y > 0$ at $\tilde H = -\frac{2}{3}\sqrt{2}$. Also note the heteroclinic saddle-saddle connection from

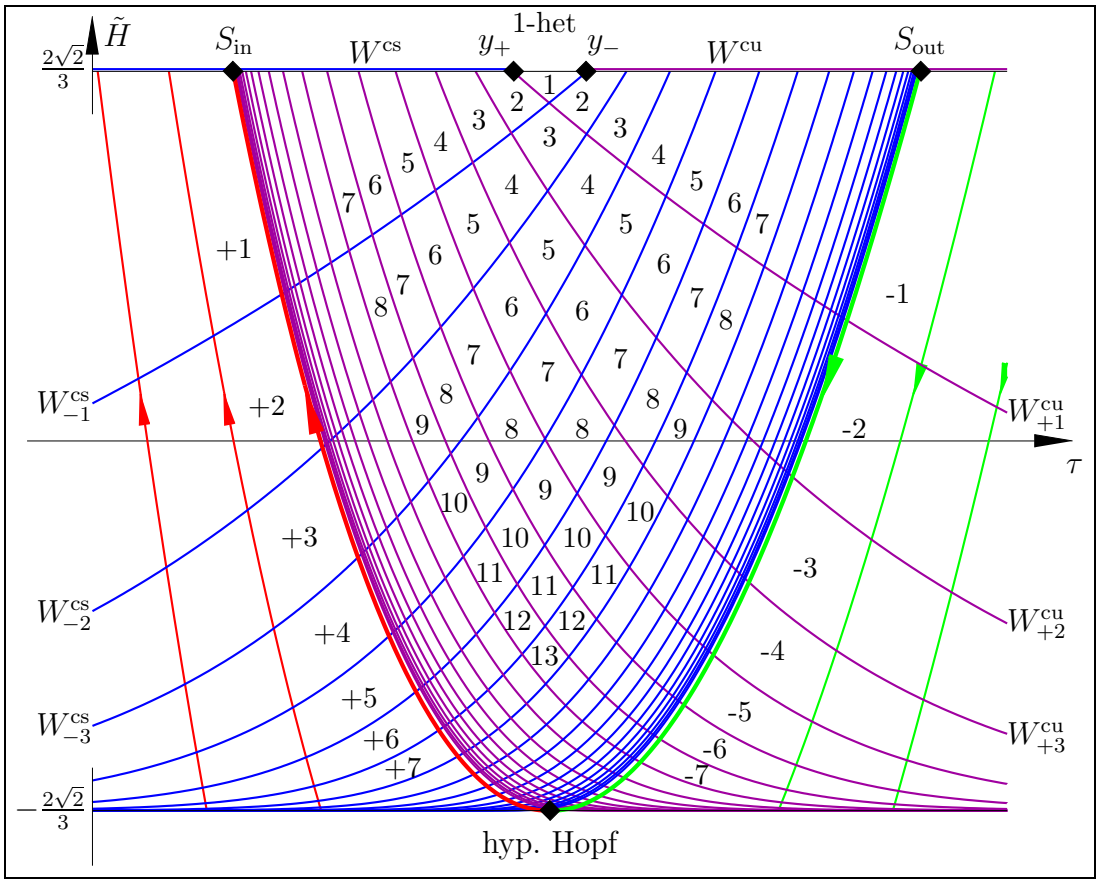

Figure 11.3: Poincaré section Σ of case (B), $\lambda > 0$ of figure 9.1. Coding: magenta = W^{cu}(saddle), blue = W^{cs}(saddle), red = W^{uu}(center), and green = W^{ss}(center).

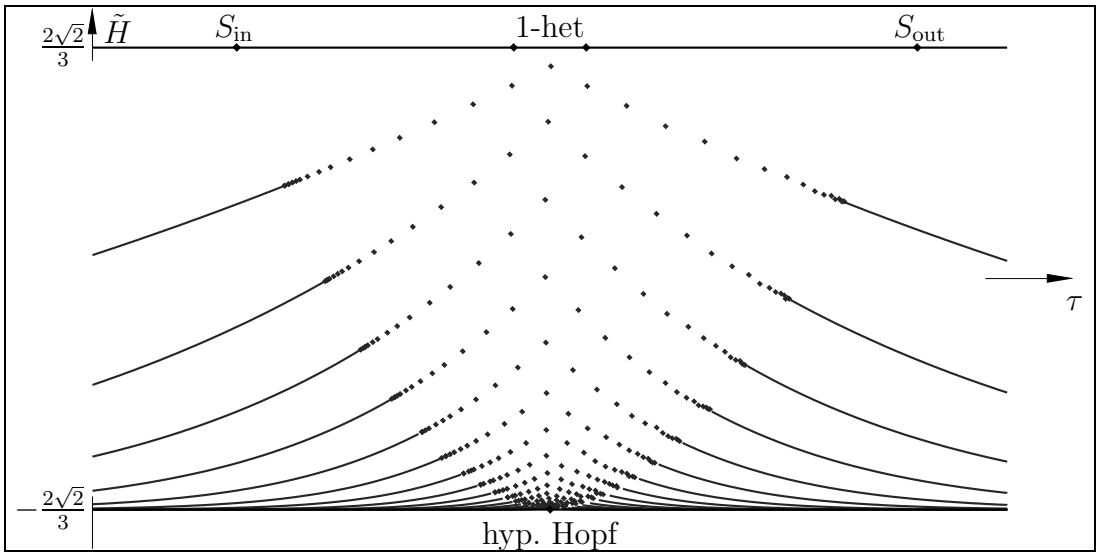

Figure 11.4: Set of bounded orbits in the Poincaré section Σ of case (B), $\lambda > 0$.

y_- to y_+ which was established in section 10.

From our analysis of the Poincaré flow in figure 9.1 (B), $\lambda > 0$, we conclude that Π^ε maps the collection W^{cu} of strong unstable manifolds of saddles to the right of y_- as is indicated by W^{cu}_{+n} in figure 11.3. Note how these manifolds W^{cu}_{+n} converge to the union of $W^{\mathrm{u}}_{\mathrm{Hopf}}$ with the bottom line of normally stable equilibria to the right of the Hopf point. A similar pattern W^{cs}_{-n} arises from the center stable manifold W^{cs} of saddles to the left of y_+ under backwards iteration of Π^ε.

By continuity of the curves W^{cu}_{+n}, $W^{\mathrm{cs}}_{-n'}$, $n, n' = 0, 1, 2, \ldots$, each curve W^{cu}_{+n} must intersect each curve W^{cs}_{-n} at least once, in the sector of Σ between $W^{\mathrm{u}}_{\mathrm{Hopf}}$ and $W^{\mathrm{s}}_{\mathrm{Hopf}}$, say at a point $y_n^{n+n'}$. Then the $(n + n' + 1)$ points $y_k^{n+n'}$, $k = 0, \ldots, n + n'$, lie on an $(n + n')$-*heteroclinic* orbit from the saddle $y_0^{n+n'}$ to the saddle $y_{n+n'}^{n+n'}$. Indeed $\Pi^\varepsilon(y_k^{n+n'}) = y_{k+1}^{n+n'}$. Note $y_- = y_0^1$, $y_+ = y_1^1$, in this notation. We call these points $(n+n')$-heteroclinic because they revolve around the equilibrium line $\mathbf{x} = 0$ for $(n + n')$ times before returning to the saddle line; see figure 6.1. Note that neither (expected) uniqueness nor transversality of these infinitely many saddle-saddle heteroclinic orbits was addressed here. We have only established their existence.

In conclusion, except for equilibria and the above $(n + n')$-heteroclinic orbits $y_k^{n+n'}$, all points in Σ leave the region U in forward or backward time, due to homoclinic splitting, see figure 11.4. In figure 11.3 we have indicated lifetimes in numbers of revolution $\pm n$, according to direction of exit. In the sector between $W^{\mathrm{u}}_{\mathrm{Hopf}}$ and $W^{\mathrm{s}}_{\mathrm{Hopf}}$ we have indicated the total number of revolutions, because the points outside $\bigcup_n (W^{\mathrm{cu}}_n \cup W^{\mathrm{cs}}_{-n})$ in this sector exit in both forward and backward time. Again we note that all nonstationary orbits which remain in U are heteroclinic, as was claimed in section 3 and in figure 3.1, including saddle-saddle $(n+n')$-heteroclinic orbits $y_k^{n+n'}$, $k = 0, \ldots, n+n'$, for any $n+n' = 1, 2, 3, \ldots$. These facts persist under higher order perturbations. In addition to the geometric insight now gained into the three different cases of Takens-Bogdanov bifurcation without parameters, these observations complete the proof of our claims of section 3.

12 Stiff hyperbolic balance laws

In this last section we return to example 1.2, (1.8)–(1.11) of hyperbolic conservation laws with stiff source terms

$$\partial_t u + \partial_\xi F(u) \;=\; \varepsilon^{-1} G(u) + \varepsilon\delta\partial_\xi^2 u, \qquad u \in \mathbb{R}^n,\ \xi \in \mathbb{R}, \tag{12.1}$$

which was mentioned in the introduction. Here $\delta \geq 0$ is a fixed small parameter providing a small viscous regularization, and $\varepsilon \searrow 0$ accounts for the stiffness of the source term. For the sake of simplicity of the following calculations we restrict ourselves to the case $\delta = 0$ of vanishing viscosity. Results for small δ can be obtained by a perturbation analysis as demonstrated in [FL00], [Lie00] for the case of Hopf bifurcation without parameters.

Rescaling $t = \tilde{t}/\varepsilon$, $\xi = \tilde{\xi}/\varepsilon$ and omitting tildes we arrive at the ε-independent system

$$\partial_t u + \partial_\xi F(u) \;=\; G(u), \qquad u \in \mathbb{R}^n,\ \xi \in \mathbb{R}. \tag{12.2}$$

Strict hyperbolicity of this balance law requires $\mathrm{D}F(u)$ to possess n distinct real eigenvalues $\alpha_1(u) < \cdots < \alpha_n(u)$ for any u. Travelling-wave solutions $u(t,\xi) = U(\xi - st)$ are given by solutions of

$$\dot{U} = \left(F'(U) - s\right)^{-1} G(U), \tag{12.3}$$

as long as $s \notin \{\alpha_1, \ldots, \alpha_n\}$. Heteroclinic orbits of (12.3) between equilibria u_-, u_+ correspond to travelling waves $u(t,\xi) = U(\varepsilon^{-1}(\xi - st))$ of (12.1) which connect the left and right states u_-, u_+ by a thin layer with width of order ε. In the limit $\varepsilon \searrow 0$ they tend to discontinuous weak solutions, called shocks.

For a system of m pure conservation laws combined with $n - m$ balance laws we expect m-dimensional equilibrium manifolds of (12.3). A different mechanism that leads to manifolds of equilibria is provided by source terms $G(u)$ which only depend on some, but not all, of the components of u. Chemical reactions, for example, typically depend on concentrations and temperature but not on flow velocities.

Aiming at Takens-Bogdanov points on such equilibrium manifolds we consider four-dimensional systems $n = 4$ with two-dimensional manifolds of vanishing source $G = 0$. We intend to provide examples of (12.3) exhibiting Takens-Bogdanov bifurcations which are generated by the *interaction* of flux F and source G. Separately, none of these components would be compatible with such complicated heteroclinic behaviour as we have observed for example near the Hopf line.

In fact, the flux can be chosen as a gradient $F(U) = \nabla_{\mathrm{U}}\Psi(U)$. Therefore the travelling wave equation that corresponds to the pure conservation law

$$\partial_t u + \partial_\xi F(u) \;=\; \varepsilon\delta\partial_\xi^2 u, \tag{12.4}$$

is of gradient type

$$\dot{U} \;=\; \nabla\Psi(U) - sU + C, \qquad C = \text{constant}\,. \tag{12.5}$$

All bounded trajectories of this system converge to equilibria, no foci occur.

The pure kinetics

$$\partial_t u \;=\; G(u), \tag{12.6}$$

on the other hand, can be chosen to be stabilizing: $G'(u)$ will possess real, negative eigenvalues, in addition to the two trivial eigenvalues generated by the manifold of equilibria. Each local trajectory of (12.6) then converges eventually monotonically to some point on the equilibrium manifold.

In contrast to their individual properties, the interaction of a gradient flux function F with a stiff, but stable, source term G in (12.1) can provide Takens-Bogdanov points with all the structure described in the preceeding sections. In particular any heteroclinic orbit that we found near the bifurcation point corresponds to a small-amplitude travelling wave of the hyperbolic balance law.

To construct our example of (12.3) with Takens-Bogdanov bifurcation at the origin, we absorb the wave speed into the flux by setting $s = 0$. We have to require $G(0) = 0$. The linearization at the origin will satisfy

$$\begin{pmatrix} 0 & 0 & 0 & 0 \\ 1 & 0 & 0 & 0 \\ 0 & 1 & 0 & 0 \\ 0 & 0 & 0 & 0 \end{pmatrix} \;=\; (F'(U))^{-1} G'(U)|_{U=0} \;=\; (F'(0))^{-1} G'(0). \tag{12.7}$$

Moreover F' must be invertible and, because $F = \nabla_{\mathrm{U}}\Psi$, symmetric. This can easily be achieved, for example by the choices

$$F'(0) \;=\; \begin{pmatrix} 0 & \gamma_1 & 0 & 0 \\ \gamma_1 & 0 & \gamma_2 & 0 \\ 0 & \gamma_2 & \gamma_3 & 0 \\ 0 & 0 & 0 & \gamma_4 \end{pmatrix}, \qquad G'(0) \;=\; \begin{pmatrix} \gamma_1 & 0 & 0 & 0 \\ 0 & \gamma_2 & 0 & 0 \\ \gamma_2 & \gamma_3 & 0 & 0 \\ 0 & 0 & 0 & 0 \end{pmatrix}, \tag{12.8}$$

with $\gamma_1, \gamma_2 < 0$ and $\gamma_3, \gamma_4 \neq 0$. The following example provides an expansion at the origin which directly coincides with the normal form (3.9), by the identification $u =$

$(u_1, u_2, u_3, u_4) = (x_1, x_2, y_1, y_2)$:

$$\begin{aligned} F(u) &= \nabla_{\mathrm{u}}\Psi(u) \\ \Psi(u) &= \gamma_1 u_1 u_2 + \gamma_2 u_2 u_3 + \tfrac{1}{2}\gamma_3 u_3^2 + \tfrac{1}{2}\gamma_4 u_4^2 \\ G(u) &= F'(u)\cdot(\text{normal form}) \\ &= \begin{pmatrix} \gamma_1 u_1 \\ \gamma_2 u_2 + \gamma_1(-u_3+u_4)u_1 - \gamma_1 u_3 u_2 + \gamma_1 b u_2^2 \\ \gamma_2 u_1 + \gamma_3 u_2 \\ 0 \end{pmatrix} \end{aligned} \tag{12.9}$$

Although the flux F is linear in this example, (12.9) meets all requirements for Takens-Bogdanov bifurcation discussed before. Similar examples with genuinely nonlinear flux functions F can be constructed by choosing a genuinely nonlinear F with linearization (12.8) at the origin and setting $G = F \cdot (\text{normal form})$, as above. With the parameter choices

$$\gamma_1 = -\sqrt{6}, \quad \gamma_2 = -5, \quad \gamma_3 = 6, \quad \gamma_4 = -1, \tag{12.10}$$

for example, $G'(0)$ possesses eigenvalues $-5,-\sqrt{6},0,0$ and $F'(0)$ possesses eigenvalues $-4,-1,+1,+9$ such that G is stabilizing the origin and F is strictly hyperbolic. Note that this structure will persist under small changes of the parameters as well as under small changes of the wave speed s.

In summary, Takens-Bogdanov bifurcations are possible in stiff hyperbolic balance laws of the form (12.1). This holds true for genuinely nonlinear flux F, nonvanishing viscosity $\delta > 0$, and under small perturbations of the system. We conclude by highlighting some of those properties of the shock solutions generated by our Takens-Bogdanov example which contradict conventional wisdom for small amplitude shocks of systems of nonlinear, strictly hyperbolic balance laws.

For hyperbolic conservation laws one usually expects viscous shock profiles to be monotone. In particular, in numerical simulations small oscillations near the shock layer are regarded as numerical artefacts due to grid phenomena or unstable numerical schemes. In many schemes "numerical viscosity" is used to automatically suppress such oscillations as "spurious". Near Takens-Bogdanov points, in contrast, all heteroclinic orbits with asymptotic states near the Hopf line correspond to travelling waves with necessarily oscillatory tails. Near elliptic Hopf points, see case (C) of figure 3.1, both tails are oscillatory. In all cases (A-C), any heteroclinic connection between the left and right side of the curve $y^2 - 2(\lambda+2)y + \lambda^2 = 0$ of vanishing discriminant, in figure 3.1, gives rise to a travelling wave solution of (12.2) with only one oscillatory tail. These oscillations are generated by the complex eigenvalues of the linearization (3.6) near the Hopf line. In figure 12.1 a

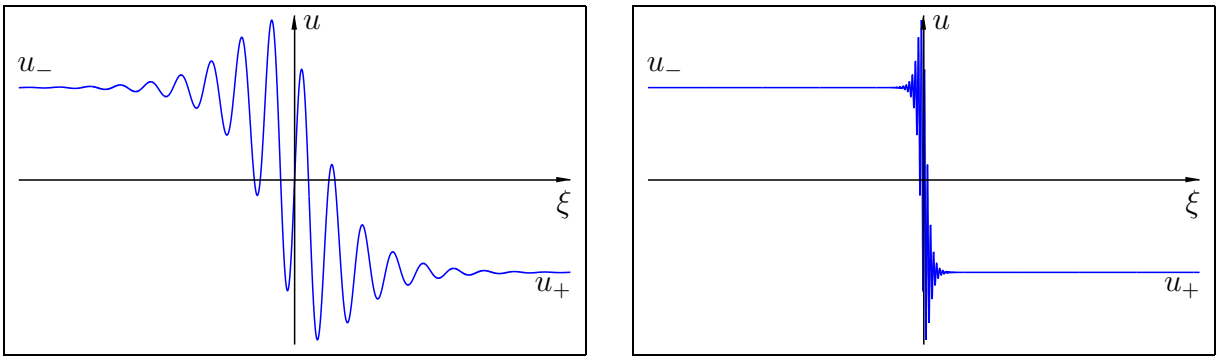

Figure 12.1: oscillatory profile in the singular limit $\varepsilon \searrow 0$.

travelling wave with oscillatory tails in the limit $\varepsilon \searrow 0$ of the stiff source is sketched. The oscillations near the shock layer resemble the Gibbs phenomenon, but in our case they are an intrinsic property of the solution. Numerical schemes should therefore resolve this "overshoot" rather than suppress it.

A second paradigm of strictly hyperbolic conservation laws is the Lax admissibility criterion. An admissible shock must have a speed s, such that exactly one characteristic family i is absorbed in the shock. In terms of the eigenvalues $\alpha_i(u)$ of $\mathrm{D}F(u)$ the Lax criterion reads

$$\begin{array}{ccccccc} \alpha_1 < \cdots < \alpha_{i-1}(u_-) & < & s & < & \alpha_i & (u_-) < \cdots < \alpha_n \\ \alpha_1 < \cdots < \alpha_i & (u_+) & < & s & < & \alpha_{i+1}(u_+) < \cdots < \alpha_n \end{array} \tag{12.11}$$

For weak shocks of hyperbolic conservation laws the Lax criterion is also a structural stability criterion for the heteroclinic connection of the corresponding travelling wave equation. See [Smo94] for more background on shock waves of hyperbolic conservation laws. In our situation, in contrast, the shock speed is determined by the interaction of flux F *and* source $\varepsilon^{-1}G$. Specifically, the order of the eigenvalues $\alpha_1, \ldots, \alpha_n$ of the flux F and the wave speed s turns out to be the same at both asymptotic states of all small-amplitude heteroclinic orbits near the Takens-Bogdanov bifurcation. Takens-Bogdanov points can be constructed for arbitrary relations of characteristic speeds α_i and wave speed s.

In [Lie00] a PDE stability analysis for oscillatory connections near elliptic Hopf points (along lines of equilibria) was carried out for systems of the form (12.1). It turned out that oscillatory waves of extreme speed, i.e. of speeds faster or slower than all characteristic speeds, are convectively stable: they are linearly stable in an appropriate exponentially weighted space. Waves of intermediate speeds, in contrast, cannot be stabilized by any exponential weight. Near Takens-Bogdanov points, however, the PDE stability analysis of saddle-saddle and of saddle-center shock profiles remains open.

13 Appendix: Derivation of the normal form

In this appendix we sketch a derivation of the normal form (4.13). Our derivation is semi-elementary; we use the scalar product from [ETB+87] as presented in [Van89]. More sophisticated results on normal forms for nilpotent linear parts, based on $SL(2,\mathbb{R})$-representations are available in [CS86], [Mur98], [Mur01]. These methods have not yet been adapted to the constraints imposed by equilibrium planes and will not be required for our specific analysis.

We derive the normal form (4.13) in three consecutive steps. Based on the crucial observation

$$(\operatorname{ad} A)^{\mathrm{T}} \;=\; \operatorname{ad}(A^{\mathrm{T}}), \tag{13.1}$$

which holds for the scalar product on polynomials, introduced in [ETB+87], we first derive the normal form

$$\begin{aligned} \dot{x}_1 &= h_1 x_1 + h_2 x_2 + h_3 x_2^2 \\ \dot{x}_2 &= x_1 + h_1 x_2 + h_{2,0} y_1 + 2 h_3 x_2 y_1 \\ \dot{y}_1 &= x_2 + h_{1,0} y_1 + 2 h_{3,0} y_1^2 \\ \dot{y}_2 &= h_4 \pi \end{aligned} \tag{13.2}$$

see (13.13)–(13.34). Here $h_j = h_j(\pi, \mathbf{y})$, where $\pi := x_2^2 - 2x_1 y_1$, and $h_{j,0}(\pi, \mathbf{y}) := h_j(\pi, \mathbf{y}) - h_j(0, \mathbf{y})$. Moreover $h_1(0,0) = h_2(0,0) = 0$ to avoid additional linear terms. In proposition 13.2 below we show that π, $\mathbf{y}$ are generating the ring of polynomials $\psi(z)$ in $z = (\mathbf{x}, \mathbf{y})$ which are invariant under $\exp(A^{\mathrm{T}} t)$. The nonlinear terms on the right-hand side of (13.2) are now complementary to the range of $\operatorname{ad}(A)$.

In a second step, we add a suitable element of $\operatorname{range}\operatorname{ad}(A)$ to convert the normal form (13.2) to the normal form

$$\begin{aligned} \dot{x}_1 &= h_1 x_1 + h_2 x_2 + h_3 x_2^2 \\ \dot{x}_2 &= x_1 \\ \dot{y}_1 &= x_2 \\ \dot{y}_2 &= h_4 \pi \end{aligned} \tag{13.3}$$

see (13.35)–(13.44). Note how the third order structure in y_1 appears, which was so crucial to our analysis. Again $h_j = h_j(\pi, \mathbf{y})$ and $h_1(0,0) = h_2(0,0) = 0$.

In a final step, we slightly massage the term h_4 to obtain the form (4.13), which is more suitable for the linear substitution (4.15), on the level of second order terms; see (13.45)–(13.49).

As a prerequisite for our derivation of the normal form (13.2), related to $\ker \operatorname{ad} A^{\mathrm{T}}$,

we collect some elementary facts. Define the linear differential operators D, D_* by

$$\begin{aligned} D &:= x_2\partial_{y_1} + x_1\partial_{x_2}, \\ D_* &:= x_2\partial_{x_1} + y_1\partial_{x_2}. \end{aligned} \tag{13.4}$$

Then we can rewrite

$$(\operatorname{ad} A)g = \begin{pmatrix} 0 \\ g_1 \\ g_2 \\ 0 \end{pmatrix} - Dg, \qquad (\operatorname{ad} A^{\mathrm{T}})H = \begin{pmatrix} H_2 \\ H_3 \\ 0 \\ 0 \end{pmatrix} - D_*H, \tag{13.5}$$

with $g = (g_1, g_2, g_3, g_4)$, $H = (H_1, H_2, H_3, H_4)$. Note that y_2 does not appear in D, D_* neither as coefficient nor as differential. Since we are interested in kernels and ranges of $\operatorname{ad} A$, $\operatorname{ad} A^{\mathrm{T}}$ in certain subspaces of polynomials, we can therefore suppress the invariant y_2, notationally, and derive the normal form for the part $z = (x_1, x_2, y_1)$, only, which exhibits the more interesting nilpotency of A of order 3.

Proposition 13.1

(i) $Dy_1 = x_2, \quad Dx_2 = x_1, \quad Dx_1 = 0,$

(ii) $D_*x_1 = x_2, \quad D_*x_2 = y_1, \quad D_*y_1 = 0,$

(iii) $D\pi = D_*\pi = 0, \quad$ *for* $\pi = x_2^2 - 2x_1y_1.$

Proof. The proof is trivial, but benefits from the observation that an interchange of x_1 and y_1 converts D, D_* into each other. ⋈

Proposition 13.2 *Let $\psi = \psi(x_1, x_2, y_1)$ be a polynomial, $\pi = x_2^2 - 2x_1y_1$.*

(i) Euclidean algorithm: there exist polynomials $\tilde\psi(x_1, x_2, y_1)$, $r_0(x_1, y_1)$, $r_1(x_1, y_1)$ such that

$$\psi = \tilde\psi\pi + r_1x_2 + r_0 \tag{13.6}$$

(ii) Let ψ be invariant under $\exp(A^{\mathrm{T}}t)$, that is $\psi(\exp(A^{\mathrm{T}}t)z) = \psi(z)$ for all z or, equivalently, $D_*\psi(z) = 0$. Then

$$\psi(z) = h(\pi, y_1), \tag{13.7}$$

for some polynomial h. In particular, y_1 and π generate the ring of $\exp(A^{\mathrm{T}}t)$-invariants (y_2 is suppressed).

Proof. Claim (i) follows from the Euclidean algorithm with respect to x_2. Note that r_0, r_1, $\tilde\psi$ are indeed polynomials in (x_1, x_2, y_1), rather than rational functions, because x_2^2 appears with coefficient 1 in π.

To proof claim (ii), let $z(t) = (\frac{1}{2}t^2y_1, ty_1, y_1)$ be the $\exp(A^{\mathrm{T}}t)$-orbit of $z(0) = (0,0,y_1)$. Then

$$\tfrac{\mathrm{d}}{\mathrm{d}t}\psi(z(t)) \;=\; D_*\psi(z(t)) \;=\; 0 \tag{13.8}$$

and hence $\psi_0(z) := \psi(z) - \psi(0,0,y_1)$ satisfies

$$\psi_0(z(t)) \;\equiv\; 0 \tag{13.9}$$

for all t. We now apply the Euclidean algorithm (i) to ψ_0 and obtain a polynomial identity

$$\psi_0(z) \;=\; \tilde{\psi}_0\pi + r_1x_2 + r_0. \tag{13.10}$$

Both ψ_0 and π vanish for all $z(t)$. Therefore

$$r_1(\tfrac{1}{2}t^2y_1, y_1)\cdot ty_1 + r_0(\tfrac{1}{2}t^2y_1, y_1) \;=\; 0 \tag{13.11}$$

for all t, y_1. Writing (13.11) as a polynomial in t with coefficients which are polynomials in y_1, we see that coefficients vanish for even and odd orders in t, alike. Hence $r_0 = r_1 = 0$, and (13.10) implies

$$\psi(z) \;=\; \psi(0,0,y_1) + \pi\tilde{\psi}_0(z). \tag{13.12}$$

Repeating this process, with $\tilde{\psi}_0$ replacing ψ, proves (13.7) and claim (ii). ⋈

To derive normal forms we introduce the following spaces of vector polynomials in $z = (\mathbf{x}, \mathbf{y})$

$$\begin{aligned} W &= \{f(z) \mid f(0,\mathbf{y}) = 0 \ \text{ for all } \mathbf{y}\} \\ V &= \{g(z) \mid g^{\mathbf{x}}(0,\mathbf{y}) = 0 \ \text{ for all } \mathbf{y}\} \\ V_c &= \{c(y) \mid c^{\mathbf{y}} \equiv 0\}. \end{aligned} \tag{13.13}$$

Clearly $V \oplus V_c$ span all polynomials. By assumption, our original vector field $f(z) \in W$ fixes the equilibrium plane $\{\mathbf{x} = 0\}$. Our normal form transformation $g(z)$ is taken from V; see (4.12). Observe that

$$\operatorname{ad} A \;:\; V \longrightarrow W \subseteq V, \tag{13.14}$$

either by direct calculation, or by contemplating that our normal form transformations leave the equilibrium plane invariant. Normal forms are therefore given by a complement to $\operatorname{range}(\operatorname{ad} A)|_V$ within W. With respect to the scalar product of [ETB+87] we have

$$(\operatorname{range}\operatorname{ad} A)^{\perp} \;=\; \ker\operatorname{ad} A^{\mathrm{T}} \tag{13.15}$$

in the total space $V \oplus V_c$. In our restricted situation, an orthogonal complement to $\operatorname{range}(\operatorname{ad} A)|_V$ in W is therefore given by

$$H \;\in\; \left((\operatorname{ad} A^{\mathrm{T}})|_W\right)^{-1}(V_c). \tag{13.16}$$

In coordinates $H = (H_1, \ldots, H_4)$ this means that

$$(\operatorname{ad} A^{\mathrm{T}})H \;=\; \begin{pmatrix} H_2 - D_*H_1 \\ H_3 - D_*H_2 \\ -D_*H_3 \\ -D_*H_4 \end{pmatrix} \;=\; \begin{pmatrix} c_1(\mathbf{y}) \\ c_2(\mathbf{y}) \\ 0 \\ 0 \end{pmatrix} \tag{13.17}$$

for $H \in W$ and suitably polynomials c_1, c_2. For example, $D_*H_4 = 0$ and proposition 13.2 (ii), applied to H_4 instead of ψ, immediately implies the normal form

$$\dot{y}_2 \;=\; H_4(z) \;=\; h(\pi, \mathbf{y}) \;=\; h_4(\pi, \mathbf{y})\pi \tag{13.18}$$

as was claimed in (13.3). Indeed, $H \in W$ implies $h(0, \mathbf{y}) = H_4(0, \mathbf{y}) = 0$ for all $\mathbf{y}$.

With such encouragement around, we now return to suppressing y_2 entirely. The first three components of (13.17) imply

$$D_*^3 H_1 \;=\; 0 \tag{13.19}$$

because $D_*y_1 = 0$ and, henceforth suppressed, $D_*y_2 = 0$. Conversely, any solution of (13.19) generates a unique solution of (13.17) by

$$\begin{aligned} H_2 &:= D_*H_1 + c_1(y_1) \\ H_3 &:= D_*H_2 + c_2(y_1). \end{aligned} \tag{13.20}$$

Indeed, $c_1(y_1)$ and $c_2(y_1)$ are determined by $H \in W$ to be given by $-D_*H_1$, $-D_*H_2$, respectively, evaluated at $z = (0, 0, y_1)$.

Lemma 13.3 *Let $\psi = \psi(x_1, x_2, y_1)$ be any polynomial such that $D_*^3\psi = 0$. Then*

$$\psi \;=\; \tilde{h}_0 + \tilde{h}_1 x_1 + \tilde{h}_2 x_2 \tag{13.21}$$

for some $\exp(A^{\mathrm{T}}t)$-invariant polynomials $\tilde{h}_j = \tilde{h}_j(\pi, y_1)$, $\pi = x_2^2 - 2x_1y_1$. Conversely, any polynomial (13.21) satisfies $D_*^3\psi = 0$.

Proof. Since $D_*y_1 = D_*\pi = 0$, by proposition 13.1, the converse part follows trivially from

$$D_*^3 x_1 \;=\; D_*^2 x_2 \;=\; D_* y_1 \;=\; 0. \tag{13.22}$$

Now suppose $D_*^3\psi = 0$. With $z(t) := (\frac{1}{2}t^2y_1, ty_1, y_1)$ as before, and the abbreviation $\psi(t) = \psi(z(t))$ we obtain

$$\dddot{\psi}(t) \;=\; D_*^3\psi(z(t)) \;=\; 0 \tag{13.23}$$

and therefore

$$\psi(t) \;=\; \psi(0) + \dot{\psi}(0)t + \tfrac{1}{2}\ddot{\psi}(0)t^2. \tag{13.24}$$

Obviously, the time-derivatives at $t = 0$ satisfy

$$\begin{aligned} \psi(0) &= \psi, \\ \dot\psi(0) &= D_*\psi = y_1\partial_{x_2}\psi, \\ \ddot\psi(0) &= D_*^2\psi = y_1\partial_{x_1}\psi + y_1^2\partial_{x_2}\psi, \end{aligned} \tag{13.25}$$

with right-hand sides evaluated at $(0, 0, y_1)$. Inserting into (13.24) implies

$$\psi(t) = a_0 + a_2y_1t + a_1\tfrac{1}{2}y_1t^2 = a_0 + a_1x_1(t) + a_2x_2(t) \tag{13.26}$$

for suitable polynomials $a_j = a_j(y_1)$. Now consider

$$\psi_0(z) := \psi(z) - a_0 - a_1x_1 - a_2x_2 \tag{13.27}$$

and apply the Euclidean algorithm of proposition 13.2, as in (13.9)–(13.12) above. Indeed

$$\psi_0(z(t)) = 0 \tag{13.28}$$

by construction, and

$$\psi_0 = \tilde\psi_0\pi + r_1x_2 + r_0 \tag{13.29}$$

imply $r_0 = r_1 = 0$, as before. This implies

$$\psi(z) = a_0 + a_1x_1 + a_2x_2 + \pi\tilde\psi_0(z). \tag{13.30}$$

Moreover, and most importantly

$$\pi D_*^3\tilde\psi_0(z) = D_*^3\psi(z) = 0 \tag{13.31}$$

for all z, and hence $D_*^3\tilde\psi_0(z) = 0$ because $a_j = a_j(y_1)$. This enables us to repeat the process, with $\tilde\psi_0$ replacing ψ. This proves the form (13.21) of ψ, and the lemma. ⋈

We are now ready to prove the $(\dot x_1, \dot x_2, \dot y_1)$-part of the normal form (13.2). Since $D_*^3H_1 = 0$, by (13.19), and since $H \in W$, lemma 13.3 applied to $\psi := H_1$ implies

$$\begin{aligned} \dot x_1 = H_1 &= \tilde h_0\pi + \tilde h_1x_1 + \tilde h_2x_2 \\ &= (\tilde h_1 - 2\tilde h_0y_1)x_1 + \tilde h_2x_2 + \tilde h_0x_2^2 \\ &= h_1x_1 + h_2x_2 + h_3x_2^2 \end{aligned} \tag{13.32}$$

with obvious definitions of h_j. Note that indeed $\tilde h_0$ can be replaced by $\tilde h_0\pi$, in (13.21), because $H \in W$ vanishes whenever $\mathbf{x} = 0$. Moreover $h_1(0, 0) = h_2(0, 0) = 0$ to ensure higher order of H_1.

With the abbreviation $h_{j,0}(\pi, y_1) := h_j(\pi, y_1) - h_j(0, y_1)$, (13.20), (13.32), proposition 13.1 and $H \in W$ together imply

$$\begin{aligned} H_2 &= D_* H_1 + c_1(y_1) \\ &= h_1 x_2 + 2h_3 x_2 y_1 + h_2 y_1 + c_1(y_1) \\ &= (h_1 + 2h_3 y_1) x_2 + h_{2,0} y_1. \end{aligned} \tag{13.33}$$

Note that in fact $h_{2,0} = \pi \cdot \hat{h}_{2,0}$, for some polynomial $\hat{h}_{2,0}$, because we have $h_{2,0}(0, y_1) = 0$ for all y_1. Similarly

$$H_3 = D_* H_2 + c_2(y_1) = h_{1,0} y_1 + 2h_{3,0} y_1^2. \tag{13.34}$$

Reinserting y_2 in all h_j the normal form (13.2) is proved.

To prove normal form (13.3), we add a suitable element $(\operatorname{ad} A)g$, $g \in V$, to H to annihilate the terms H_2 and H_3. Specifically,

$$(\operatorname{ad} A)g + H = \begin{pmatrix} -Dg_1 + H_1 \\ g_1 - Dg_2 + H_2 \\ g_2 - Dg_3 + H_3 \\ -Dg_4 + H_4 \end{pmatrix}. \tag{13.35}$$

With the choices $g_3 = g_4 = 0$, we obtain the conditions

$$\begin{aligned} g_2 &:= -H_3 \\ g_1 &:= -H_2 + Dg_2 = -H_2 - DH_3. \end{aligned} \tag{13.36}$$

The new normal form then reads

$$\begin{aligned} \dot{x}_1 &= H_1 - Dg_1 \\ \dot{x}_2 &= x_1 \\ \dot{y}_1 &= x_2 \\ \dot{y}_2 &= H_4 \end{aligned} \tag{13.37}$$

To study the transition from (13.2) to (13.3), alias (13.37), we introduce the spaces

$$\begin{aligned} \mathcal{H}_1 &:= \{H_1(0, y_1) = 0\} \cap \ker D_*^3 \\ \mathcal{H}_* &:= ((\operatorname{ad} A^{\mathrm{T}})|_W)^{-1}(V_c) \end{aligned} \tag{13.38}$$

see (13.19), (13.16). We conveniently restrict these spaces to homogeneous polynomials of fixed degree $N > 2$ in the variables $z = (x_1, x_2, y_1)$, with y_2 suppressed. Note the linear lifting isomorphism

$$\Lambda : \mathcal{H}_1 \longrightarrow \mathcal{H}_*, \tag{13.39}$$

$\Lambda(H_1) := (H_1, H_2, H_3)$ with H_2, H_3 given by the construction (13.20) of the normal form (13.2) from H_1. We claim, and show below, that the map $\Gamma(H_1, H_2, H_3) := H_1 - Dg_1$ with g_1 given by the normal form transformation (13.36) above in fact defines another linear isomorphism

$$\Gamma \;:\; \mathcal{H}_* \longrightarrow \mathcal{H}_1. \tag{13.40}$$

This proves normal form (13.3), because indeed (13.37) then takes the form

$$\begin{aligned} \dot{x}_1 &= h_1 x_1 + h_2 x_2 + h_3 x_2^2 \\ \dot{x}_2 &= x_1 \\ \dot{y}_1 &= x_2 \\ \dot{y}_2 &= h_4 \end{aligned} \tag{13.41}$$

and all invariants $h_j = h_j(\pi, \mathbf{y})$ are admissible.

It now remains to prove that Γ indeed maps $\mathcal{H}_*$ to $\mathcal{H}_1$ and that Γ possesses trivial kernel. The latter fact is obvious, because the normal form transformation is given by

$$H \;\mapsto\; H + (\operatorname{ad} A)g \tag{13.42}$$

with $(\operatorname{ad} A)g$ orthogonal to $H \in \mathcal{H}_*$, and Γ only omits components of the right-hand side of (13.42) which are already zero by construction of g.

To prove $\Gamma(H) = H_1 - Dg_1 \in \mathcal{H}_1$, we use (13.36) to explicitly compute the correction

$$Dg_1 \;=\; -DH_2 - D^2 H_3. \tag{13.43}$$

In view of definition (13.38) of $\mathcal{H}_1$ and the characterization of $\mathcal{H}_1$ by lemma 13.3 and (13.32), it is sufficient to show that both DH_2 and D^2H_3 are sums of monomials of the form

$$\pi^j y_1^k x_1, \qquad \pi^j y_1^k x_2, \qquad \pi^j y_1^{k-1} x_2^2. \tag{13.44}$$

Since $D\pi = 0$, by proposition 13.1, we may as well suppress π entirely, treating π as a coefficient in this computation.

To treat the term DH_2 in (13.43) we observe that H_2 itself contains only monomials y_1^{k+1}, $y_1^k x_2$; see (13.33). Applying $D = x_2\partial_{y_1} + x_1\partial_{x_2}$ only produces terms (13.44) from these.

To treat the term D^2H_3 in (13.43) we observe that H_3 itself contains only monomials y_1^{k+1}; see (13.34). Applying D once only produces terms $y_1^k x_2$. The second application of D generates terms $y_1^k x_1, y_1^{k-1} x_2^2$ which are already in the list (13.44). These simple observations complete our proof of normal form (13.3).

As a final step, we slightly massage the term

$$h_4\pi \;=\; \pi h_4(\pi, y_1) \tag{13.45}$$

in (13.3) to obtain the form

$$\hat{h}_4 x_1 y_1 \;=\; x_1 y_1 \hat{h}_4(x_1 y_1, y_1) \tag{13.46}$$

which the $\dot{y}_2$-term takes in (4.13). As in (13.5), (13.42), a massage is defined as addition of $-Dg_4$ such that

$$h_4\pi - Dg_4 \;=\; \hat{h}_4 x_1 y_1. \tag{13.47}$$

Clearly the spaces of polynomials of fixed degree N in $z = (x_1, x_2, y_1)$ which take the forms (13.45), (13.46), respectively, are of equal dimension. Our construction of g will depend linearly on h_4 and, by orthogonality, will define a linear isomorphism between spaces of equal dimension.

We construct g for each monomial $x_1^j x_2^{2k} y_1^\ell$, separately. First note that $D = x_2\partial_{y_1} + x_1\partial_{x_2}$ implies

$$x_1^j x_2^{2k} y_1^\ell - \tfrac{1}{\ell+1} D(x_1^j x_2^{2k-1} y_1^{\ell+1}) \;=\; \tfrac{2k-1}{\ell+1} x_1^{j+1} x_2^{2k-2} y_1^{\ell+1} \tag{13.48}$$

for $j, \ell \geq 0$ and $k \geq 1$. Subtraction of a term Dg has thus reduced the x_2-exponent by two. Iterating this procedure k times, and starting at x_1-exponent $j = 0$, we obtain g_4 such that

$$x_2^{2k} y_1^\ell - Dg_4 \;=\; c_0\,(x_1 y_1)^k y_1^\ell. \tag{13.49}$$

Since x_2 occurs only in even powers in $\pi = x_2^2 - 2x_1 y_1$ and in $h_4\pi$, this construction of g_4, which depends linearly on h_4, allows us to eliminate all (even) powers x_2^{2k} and replace them by terms $(x_1 y_1)^k$, as was required in (13.47). This finally proves our normal form (4.13), to arbitrary finite order.

References

[AA86] J. C. Alexander and G. Auchmuty. Global bifurcation of phase-locked oscillators. *Arch. Rational Mech. Anal.*, **93**:253–270, 1986.

[AF89] J. Alexander and B. Fiedler. Global decoupling of coupled symmetric oscillators. In C. Dafermos, G. Ladas, and G. Papanicolaou, editors, *Differential Equations*, volume 118 of *Lect. Notes Math.*, New York, 1989. Marcel Dekker Inc.

[Arn72] V. Arnol'd. Lectures on bifurcations and versal systems. *Russ. Math. Surv.*, **27**:54–123, 1972.

[Arn83] V. Arnol'd. *Geometrical Methods in the Theory of Ordinary Differential Equations*, volume 250 of *Grundl. math. Wiss.* Springer, New York, 1983.

[Aul84] B. Aulbach. *Continuous and discrete dynamics near manifolds of equilibria*, volume 1058 of *Lect. Notes Math.* Springer, New York, 1984.

[BM61] N. Bogolyubov and Y. Mitropol'skij. *Asymptotic methods in the theory of non-linear oscillations*. Gordon and Breach Science Publ., New York, 1961.

[Bog76a] R. Bogdanov. Bifurcation of the limit cycle of a family of plane vector fields (Russian). *Trudy Semin. Im. I. G. Petrovskogo*, **2**:23–36, 1976.

[Bog76b] R. Bogdanov. Versal deformation of a singularity of a vector field on the plane in the case of zero eigenvalues (Russian). *Trudy Semin. Im. I. G. Petrovskogo*, **2**:37–65, 1976.

[Bog81a] R. Bogdanov. Bifurcation of the limit cycle of a family of plane vector fields (English). *Sel. Mat. Sov.*, **1**:373–387, 1981.

[Bog81b] R. Bogdanov. Versal deformation of a singularity of a vector field on the plane in the case of zero eigenvalues (English). *Sel. Mat. Sov.*, **1**:389–421, 1981.

[BR01] H. Broer and R. Roussarie. Exponential confinement of chaos in the bifurcation set of real analytic diffeomorphisms. This volume, 2001.

[BT89] H. Broer and F. Takens. Formally symmetric normal forms and genericity. In U. Kirchgraber and H. O. Walther, editors, *Dynamics Reported 2*, pages 39–59. Teubner & Wiley, Stuttgart, 1989.

[CH82] S.-N. Chow and J. Hale. *Methods of Bifurcation Theory.* Springer, New York, 1982.

[CS86] R. Cushman and J. Sanders. Nilpotent normal forms and representation theory in sl(2,R). In M. Golubitsky and J. Guckenheimer, editors, *Multiparameter bifurcation theory, Proc. AMS-IMS-SIAM Joint Summer Res. Conf., Arcata/Calif. 1985*, volume 56 of *Contemp. Math.*, pages 31–51. Amer. Math. Soc., 1986.

[DR98] F. Dumortier and R. Roussarie. Geometric singular perturbation theory beyond normal hyperbolicity. Preprint, 1998.

[ETB+87] C. Elphick, E. Tirapegui, M. Brachet, P. Coullet, and G. Iooss. A simple global characerization for normal forms of singular vector fields. *Phys. D*, **29**:95–127, 1987.

[Far84] M. Farkas. ZIP bifurcation in a competition model. *Nonlinear Anal., Theory Methods Appl.*, **8**:1295–1309, 1984.

[Fen77] N. Fenichel. Asymptotic stability with rate conditions, II. *Indiana Univ. Math. J.*, **26**:81–93, 1977.

[Fen79] N. Fenichel. Geometric singular perturbation theory for ordinary differential equations. *J. Diff. Eq.*, **31**:53–89, 1979.

[FL00] B. Fiedler and S. Liebscher. Generic Hopf bifurcation from lines of equilibria without parameters: II. Systems of viscous hyperbolic balance laws. *SIAM J. Math. Anal.*, **31**(6):1396–1404, 2000.

[FLA00a] B. Fiedler, S. Liebscher, and J. Alexander. Generic Hopf bifurcation from lines of equilibria without parameters: I. Theory. *J. Diff. Eq.*, **167**:16–35, 2000.

[FLA00b] B. Fiedler, S. Liebscher, and J. Alexander. Generic Hopf bifurcation from lines of equilibria without parameters: III. Binary oscillations. *Int. J. Bif. Chaos Appl. Sci. Eng.*, **10**(7):1613–1622, 2000.

[FS96] B. Fiedler and J. Scheurle. *Discretization of Homoclinic Orbits and Invisible Chaos*, volume 570 of *Mem. AMS.* Amer. Math. Soc., Providence, 1996.

[FSSW96] B. Fiedler, B. Sandstede, A. Scheel, and C. Wulff. Bifurcation from relative equilibria of noncompact group actions: Skew products, meanders, and drifts. *Doc. Math.*, **1**:479–505, 1996.

[Gel99] V. Gelfreich. A proof of the exponentially small transversality of the separatrices for the standard map. *Commun. math. Phys.*, **201**:155–216, 1999.

[GH82] J. Guckenheimer and P. Holmes. *Nonlinear Oscillations, Dynamical Systems, and Bifurcations of Vector Fields*, volume 42 of *Appl. Math. Sc.* Springer, New York, 1982.

[GL01] V. Gelfreich and V. Lazutkin. Splitting of separatrices: perturbation theory and exponential smallness. Accepted by Uspekhi, 2001.

[GSS85] M. Golubitsky, I. Stewart, and D. Schaeffer. *Singularities and Groups in Bifurcation Theory I*, volume 51 of *Appl. Math. Sc.* Springer, New York, 1985.

[GSS88] M. Golubitsky, I. Stewart, and D. Schaeffer. *Singularities and Groups in Bifurcation Theory II*, volume 69 of *Appl. Math. Sc.* Springer, New York, 1988.

[Hal63] J. Hale. *Oscillations in Nonlinear Systems.* Mac Graw – Hill, New York, 1963.

[HC64] A. Hurwitz and R. Courant. *Funktionentheorie* (German), volume 3 of *Grundl. math. Wiss.* Springer, New York, 4th edition, 1964.

[HK91] J. Hale and H. Koçak. *Dynamics and bifurcations*, volume 3 of *Texts in Appl. Math.* Springer, New York, 1991.

[HPS77] M. Hirsch, C. Pugh, and M. Shub. *Invariant Manifolds*, volume 583 of *Lect. Notes Math.* Springer, Berlin, 1977.

[Kuz95] Y. Kuznetsov. *Elements of applied bifurcation theory*, volume 112 of *Appl. Math. Sc.* Springer, New York, 1995.

[Lan87] S. Lang. *Elliptic Functions*, volume 112 of *Grad. Texts in Math.* Springer, New York, 2nd edition, 1987.

[Lie97] S. Liebscher. Stabilität von Entkopplungsphänomenen in Systemen gekoppelter symmetrischer Oszillatoren (German). Diplomarbeit, Freie Universität Berlin, 1997.

[Lie00] S. Liebscher. *Stable, Oscillatory Viscous Profiles of Weak, non-Lax Shocks in Systems of Stiff Balance Laws.* Dissertation, Freie Universität Berlin, 2000.

[Mur98] J. Murdock. Asymptotic unfoldings of dynamical systems by normalizing beyond the normal form. *J. Diff. Eq.*, **143**:151–190, 1998.

[Mur01] J. Murdock. On the structure of normal form modules. Preprint, 2001.

[Nei84] A. Neishtadt. On the separation of motions in systems with rapidly rotating phase. *J. Appl. Math. Mech.*, **48**:134–139, 1984.

[Sho75] A. Shoshitaishvili. Bifurcations of topological type of a vector field near a singular point (Russian). *Trudy Semin. Im. I. G. Petrovskogo*, **1**:279–309, 1975.

[Smo94] J. Smoller. *Shock Waves and Reaction-Diffusion Equations*, volume 258 of *Grundl. math. Wiss.* Springer, New York, 1983, 1994.

[Tak73] F. Takens. Forced oscillations and bifurcations. The Utrecht preprint, reproduced in this volume, 1973.

[Tak74] F. Takens. Singularities of vector fields. *Publ. Math., Inst. Hautes Etud. Sci.*, **43**:47–100, 1974.

[Tri37] F. Tricomi. *Funzioni ellittiche* (Italian), volume 248 of *Monogr. di mat. appl. per cura d. consiglio naz. d. ricerche.* Nicola Zanichelli, Bologna, 1937.

[Tri48] F. Tricomi. *Elliptische Funktionen. Übersetzt und bearbeitet von M. Krafft* (German). Akademische Verlagsanstalt Geest & Portig K.-G., Leipzig, 1948.

[Van89] A. Vanderbauwhede. Centre manifolds, normal forms and elementary bifurcations. In U. Kirchgraber and H. O. Walther, editors, *Dynamics Reported 2*, pages 89–169. Teubner & Wiley, Stuttgart, 1989.